

AD-A145 764

PREDICTION AND MODELING OF HELICOPTER NOISE(U)
CONSTRUCTION ENGINEERING RESEARCH LAB (ARMY) CHAMPAIGN
IL R RASPET ET AL. AUG 84 CERL-TR-N-186

1/1.

UNCLASSIFIED

F/G 20/2

NL

END

Full MS C

638



MICROCOPY RESOLUTION TEST CHART
NATIONAL BUREAU OF STANDARDS-1963-A



**US Army Corps
of Engineers**

Construction Engineering
Research Laboratory

12
CEERL

TECHNICAL REPORT N-186

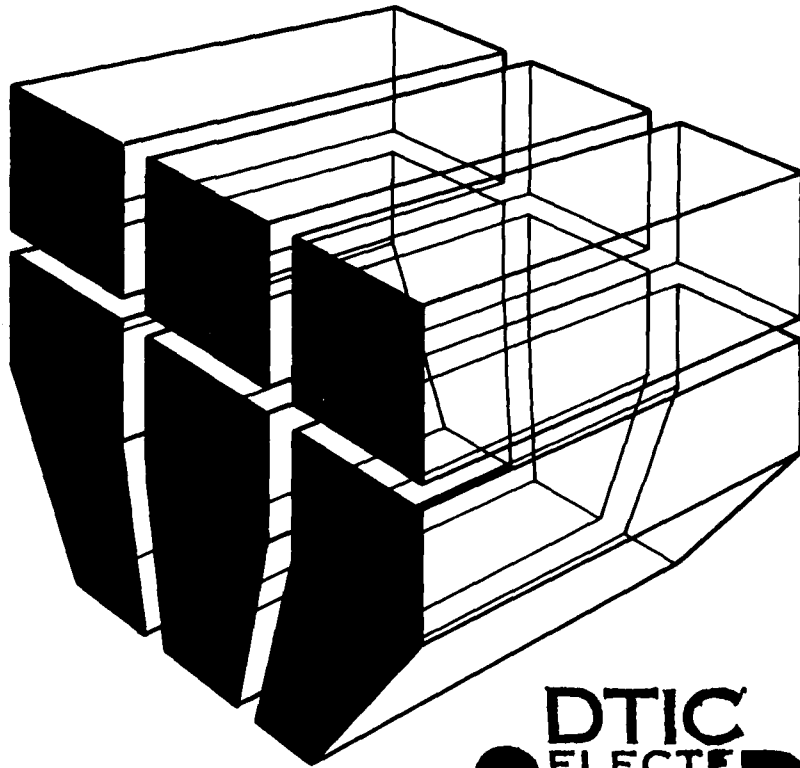
August 1984

Standard Methods to Assess Rotary-Wing Aircraft Sound Decay With Distance

PREDICTION AND MODELING OF HELICOPTER NOISE

AD-A145 764

by
**Richard Raspet
Mark Kief
Raymond Daniels**



DTIC FILE COPY

**DTIC
ELECTE**
SEP 21 1984
S D
A

Approved for public release; distribution unlimited.

9 09 20 022

The contents of this report are not to be used for advertising, publication, or promotional purposes. Citation of trade names does not constitute an official indorsement or approval of the use of such commercial products. The findings of this report are not to be construed as an official Department of the Army position, unless so designated by other authorized documents.

*DESTROY THIS REPORT WHEN IT IS NO LONGER NEEDED
DO NOT RETURN IT TO THE ORIGINATOR*

UNCLASSIFIED

SECURITY CLASSIFICATION OF THIS PAGE (When Data Entered)

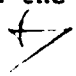
REPORT DOCUMENTATION PAGE		READ INSTRUCTIONS BEFORE COMPLETING FORM
1. REPORT NUMBER CERL-TR-N-186	2. GOVT ACCESSION NO. ADA145764	3. RECIPIENT'S CATALOG NUMBER
4. TITLE (and Subtitle) PREDICTION AND MODELING OF HELICOPTER NOISE		5. TYPE OF REPORT & PERIOD COVERED FINAL
		6. PERFORMING ORG. REPORT NUMBER
7. AUTHOR(s) Richard Raspet Mark Kief Raymond Daniels		8. CONTRACT OR GRANT NUMBER(s)
9. PERFORMING ORGANIZATION NAME AND ADDRESS U.S. Army Construction Engr Research Laboratory P.O. Box 4005 Champaign, IL 61820-1305		10. PROGRAM ELEMENT, PROJECT, TASK AREA & WORK UNIT NUMBERS 4A162720A896-A-028
11. CONTROLLING OFFICE NAME AND ADDRESS		12. REPORT DATE August 1984
		13. NUMBER OF PAGES 52
14. MONITORING AGENCY NAME & ADDRESS (if different from Controlling Office)		15. SECURITY CLASS. (of this report) UNCLASSIFIED
		15a. DECLASSIFICATION/DOWNGRADING SCHEDULE
16. DISTRIBUTION STATEMENT (of this Report) Approved for public release; distribution unlimited.		
17. DISTRIBUTION STATEMENT (of the abstract entered in Block 20, if different from Report)		
18. SUPPLEMENTARY NOTES Copies are obtainable from the National Technical Information Center Springfield, VA 22151		
19. KEY WORDS (Continue on reverse side if necessary and identify by block number) helicopters noise (sound)		
20. ABSTRACT (Continue on reverse side if necessary and identify by block number) Sound exposure level (SEL) data from three Army helicopters were used to test a proposed method for calculating sideline decay developed for fixed-wing aircraft. The Federal Aviation Administration (FAA) and the U.S. Air Force (USAF) have adopted this method for use with fixed-wing aircraft, and it was desired to know if the same method could predict rotary-wing aircraft sideline decay with distance or if a more complex computer model is necessary. The procedure was found accurate for limited altitudes and slant distances. (Cont'd)		

UNCLASSIFIED

UNCLASSIFIED

SECURITY CLASSIFICATION OF THIS PAGE(When Data Entered)

BLOCK 20. (Continued)

In addition, the sideline decay data were studied using variables known to affect sound attenuation. The purpose was to gain further insight into the mechanisms of sideline decay with distance. Variations in the results suggest an unknown mechanism is contributing to this attenuation. 

UNCLASSIFIED

SECURITY CLASSIFICATION OF THIS PAGE(When Data Entered)

FOREWORD

This work was performed by the Environmental Division (EN) of the U.S. Army Construction Engineering Research Laboratory (USA-CERL) for the Directorate of Engineering and Construction, Office of the Chief of Engineers (OCE), under Project 4A162720A896, "Environmental Quality Technology"; Technical Area A, "Installation Environmental Management Strategy"; Work Unit 028, "Standard Methods to Assess Rotary-Wing Aircraft Sound Decay With Distance." The OCE Technical Monitor was MAJ S. J. Stone, DAEN-ZCE.

Dr. R. K. Jain is Chief, EN. COL Paul J. Theuer is Commander and Director of USA-CERL, and Dr. L. R. Shaffer is Technical Director.

Accession For	
NTIS GRA&I	<input checked="checked" type="checkbox"/>
DTIC TAB	<input type="checkbox"/>
Unannounced	<input type="checkbox"/>
Justification	
By	
Distribution/	
Availability Codes	
Dist	Avail and/or Special
AI	



CONTENTS

	<u>Page</u>
DD FORM 1473	1
FOREWORD	3
LIST OF TABLES AND FIGURES	5
1 INTRODUCTION.....	7
Background	
Objectives	
Approach	
Mode of Technology Transfer	
2 PREDICTION OF HELICOPTER SIDELINE DECAY.....	9
Case 1: No Attenuation, Simple Point Source	
Case 2: Large Attenuation, Simple Point Source	
FAA/USAF Method	
3 DATA ANALYSIS AND COMPARISON WITH FAA PROCEDURE.....	13
Data Collection	
Data Reduction	
Comparative Analysis	
4 COMPUTER MODEL FOR FLYBY INTEGRATION.....	22
Attenuation Model	
Coherent Versus Incoherent: Hard Surface	
Coherent Versus Incoherent: Finite Impedence Surface	
Calculation for 305 m Altitude	
Variation in Decay Rate With Aircraft Speed	
5 DIRECTIVITY EFFECTS.....	39
Effect of Spectral Change on SEL Calculation	
Analysis of Directivity Effects on a Level Flyby	
6 FLYBY PROFILES.....	43
7 CONCLUSIONS AND RECOMMENDATIONS.....	50
REFERENCES	51
DISTRIBUTION	

TABLE

<u>Number</u>		<u>Page</u>
1	Computer-Calculated Comparison of SAE and ANSI Standards	25
FIGURES		
1	$\bar{P}_{\frac{1}{2} \text{ sec}}^2$ Versus Time for an Ideal Flyby	10
2	Geometry of a Flyby	10
3	Sideline Microphones at Fort Campbell	14
4	FAA Method Versus Measured Levels for UH-1H	16
5	FAA Method Versus Measured Levels for UH-60A	17
6	FAA Method Versus Measured Levels for CH-47C	18
7	(SEL-LEQ) Versus Distance	19
8	Comparison of Normalized A-weighted Helicopter Spectra	20
9	NHELI Program Flow Chart	24
10	Sample Output of NHELI Program	25
11	NHELI Predictions for UH-1H Over Hard Surface	26
12	NHELI Predictions for UH-60A Over Hard Surface	27
13	NHELI Predictions for CH-47C Over Hard Surface	28
14	NHELI Predictions for UH-1H Over Soft Surface	30
15	NHELI Predictions for UH-60A Over Soft Surface	31
16	NHELI Predictions for CH-47C Over Soft Surface	32
17	Soft Coherent Prediction Versus Measured Levels for UH-1H	33
18	Soft Coherent Prediction Versus Measured Levels for UH-60A	34
19	Soft Coherent Prediction Versus Measured Levels for CH-47C	35
20	Soft Coherent Prediction Versus Measured Levels for UH-1H and Normalized to 1075.4-ft (328-m) Data	37
21	Check for Variation in Decay With Speed	38
22	Spectral Variation of UH-1H Over Flyby	39

FIGURES (Cont'd)

<u>Number</u>		<u>Page</u>
23	Spectral Effects Calculation	40
24	Flyby Variation With Slant Distance	44
25	UH-1H Flyby Profile Resolved Into Frequency Bands	45
26	Temperature and Sound Speed Profile at Bondville Field Station	46
27	Temperature Profile at Fort Carson on 4 August 1982	47
28	Sound Speed Profile at Fort Carson on 4 August 1982	48
29	Refractive Attenuation at Fort Carson on 4 August 1982	48
30	Apparent Source Height at Fort Carson on 4 August 1982	49
31	Comparison of Grazing Angle for a Homogeneous Atmosphere and Fort Carson 4 August 1984 Profile	49

PREDICTION AND MODELING OF HELICOPTER NOISE

1 INTRODUCTION

Background

The Army is the largest operator of helicopters in the United States. Since helicopters often operate at low altitude, they can contribute greatly to Army installations' noise impact on surrounding land uses.

The U.S. Army Construction Engineering Research Laboratory (USA-CERL) has been studying the noise effects of rotary-wing aircraft operations for 10 years as part of the Army's Installation Compatible Use Noise Zone (ICUZ) program.¹ These studies previously have concentrated on the source characterization of Army rotary wing aircraft--the source spectra, variations in spectrum and level with speed, and variations with loading.² These source data can be combined with sideline decay predictions to assess helicopter noise impact.

The propagation models used in the earlier studies were based on contouring techniques developed for fixed-wing aircraft. Working in this area, the Federal Aviation Administration (FAA) and the U.S. Air Force (USAF) have proposed changes to the duration factor used in calculating the sideline decay of fixed-wing aircraft.³ The revised procedure should be studied to see if this change improves predictions for rotary-wing aircraft or if a more detailed model of sound propagation is necessary. Moreover, the helicopter data studied in this work--UH-1H, UH-60A, and CH-47C--could provide valuable information on the mechanics of sideline noise decay with distance.

¹Army Regulation (AR) 200-1, Environmental Protection and Enhancement (Department of the Army [DA], 15 June 1982).

²P. D. Schomer and B. L. Homans, Technical Background: Interim Criteria for Planning Rotary-Wing Aircraft Patterns and Siting Noise Sensitive Land Uses, Interim Report N-9/ADA031449 (U.S. Army Construction Engineering Research Laboratory [USA-CERL], September 1976); P. D. Schomer and B. L. Homans, User Manual: Interim Procedure for Planning Rotary-Wing Aircraft Traffic Patterns and Siting Noise Sensitive Land Uses, Interim Report N-10/ADA031450 (USA-CERL, September 1976); B. Homans, L. Little, and P. Schomer, Rotary-Wing Aircraft Operational Noise Data, Technical Report N-38/ADA051999 (USA-CERL, February 1978).

³Jerry D. Speakman, Effect of Propagation Distance on Aircraft Flyover Duration, AFAMRL-TR-81-28 (U.S. Air Force Aerospace Medical Research Laboratory, 1981); J. Steven Newman, Edward J. Rickley, and Tyrone L. Bland, Helicopter Noise Exposure Curves for Use in Environmental Impact Assessments, DOT-FAA-EE-82-16 (Department of Transportation, Federal Aviation Administration, Office of Environment and Energy, 1982).

Objectives

The objectives of this research were to:

1. Determine if the FAA procedure is accurate for predicting rotary-wing aircraft noise decay with distance
2. Examine the physical mechanisms of sideline noise decay by comparing a detailed computer model to experimental results.

The second objective had three subtasks: (a) to perform a sensitivity analysis for effects of known variables on sideline decay; (b) identify if additional mechanisms contribute to attenuation; and (c) improve standard methods of calculating the sound exposure level for rotary-wing aircraft.

Approach

Experimental data were gathered at Fort Campbell for three rotary-wing aircraft types. The measurements were taken using techniques described in detail elsewhere.⁴ The data were analyzed to give the LEQ and SEL variations with slant distance. In addition, the one-third octave spectra for each aircraft during the maximum 0.5 sec were calculated and averaged over all altitudes, microphones, and airspeeds.

Next, the experimental results for SEL versus slant distance were compared with results using the FAA method. A detailed computer model was developed that includes finite ground impedance, atmospheric attenuation, and coherent or incoherent addition of the direct and reflected sound. Results using this model were compared with those from the experiments. The effects of spectral change and directivity of the noise pattern also were studied. Finally, helicopter flyby profiles were examined to determine if an unidentified mechanism contributes to attenuation.

Mode of Technology Transfer

The information in this report will be added to USA-CERL's integrated noise contour system (INCS) database.⁵ In addition, it will be used as input to future FAA and Department of Defense Standards meetings.

⁴P. D. Schomer, A. Averbuch, and R. Raspet, Operational Noise Data for UH-60A and CH-47C Army Helicopters, Technical Report N-131/A118796 (USA-CERL, July 1982).

⁵P. D. Schomer, A. Averbuch, and R. Raspet.

2 PREDICTION OF HELICOPTER SIDELINE DECAY

The sound measurements used in studying helicopter decay are the maximum equivalent level (LEQ) and the sound exposure level (SEL). All levels are A-weighted. The LEQ is given by:

$$LEQ = 10 \log_{10} \left[\int p^2 dt / [p_o^2 \frac{1}{2}] \right], \quad [Eq 1]$$

where p_o is the reference pressure, t_o is the reference time, p is the measured pressure, and the integral is performed over the maximum noise 0.5 sec of the flyby. Figure 1 shows an ideal flyby. The SEL is given by:

$$SEL = 10 \log_{10} \frac{\int_a^b p^2 dt}{p_o^2 t_o}, \quad [Eq 2]$$

where $p_o = 20 \mu Pa$ and $t_o = 1$ sec. The integral is performed from the time the instantaneous level is 10 dB below the maximum level (a in Figure 1) until the level is again 10 dB below the maximum level (b in Figure 1).

A look at two ideal cases and the present FAA procedure will help explain the objectives. The first simple case is a flyby with no atmospheric attenuation and the second is one with a large exponential attenuation.

Case 1: No Attenuation, Simple Point Source

Model the helicopter as a simple sound source. Consider a helicopter flyby according to the geometry of Figure 2.

The SEL(D') at any slant distance D' is given by:

$$SEL(D') = SEL(D) + LEQ(D') - LEQ(D) + 10 \log (D'/D), \quad [Eq 3]$$

where $LEQ(D')$ is determined from:

$$LEQ(D') = 10 \log_{10} \sum_{n=0}^{44} 10^{[L_{\frac{1}{3}}(n)/10]} - 20 \log_{10} (D'/D), \quad [Eq 4]$$

where $L_{\frac{1}{3}}(n)$ are the one-third-octave band levels at the reference distance D . The term $10 \log (D'/D)$ is called the "duration factor" and adjusts for the difference in decay with distance of the LEQ and SEL.

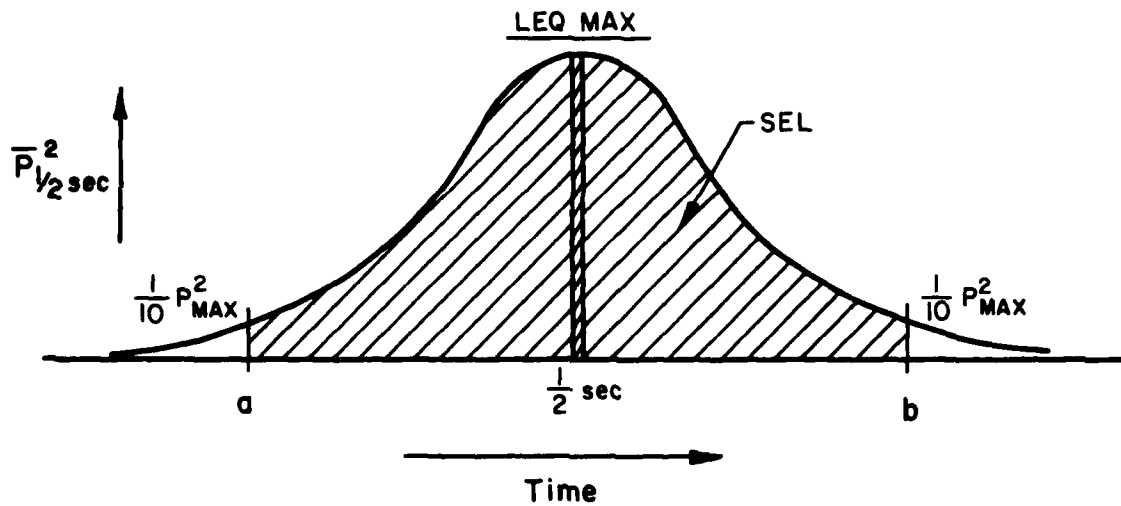


Figure 1. $\overline{P}_{1/2 \text{ sec}}^2$ versus time for an ideal flyby.

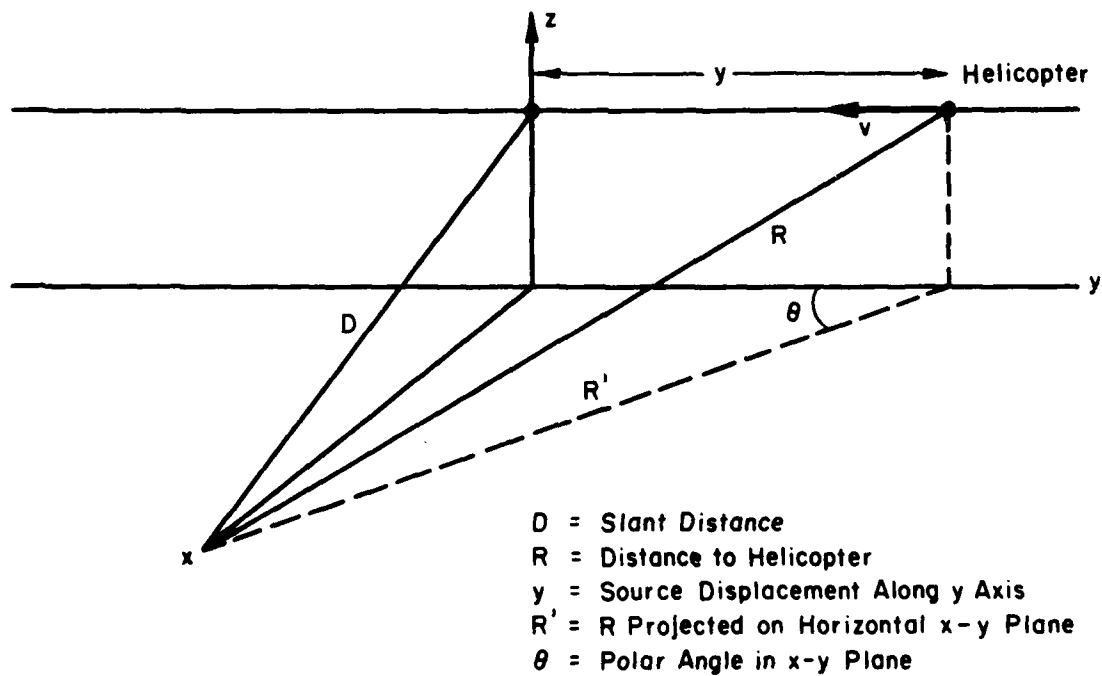


Figure 2. Geometry of a flyby.

Case 2: Large Attenuation, Simple Point Source

In the other extreme, large atmospheric attenuation, it can be shown that the factor relating the maximum LEQ and the SEL approaches $5 \log (D'/D)$. That is:

$$SEL(D') = SEL(D) + LEQ(D') - LEQ(D) + 5 \log_{10}(D'/D), \quad [Eq 5]$$

where:

$$LEQ(D') = 10 \log_{10} \sum_n 10^{[L \frac{1}{3}(n) - \alpha(n)(D'-D)]/10} - 20 \log_{10}(D'/D) \quad [Eq 6]$$

Pure exponential decay with no distance factor also gives a duration factor of 5 dB per decade.

FAA/USAF Method

The FAA/USAF standard for calculating the SEL of fixed-wing aircraft flybys modifies this distance factor to fit the data empirically. This procedure calculates the SEL by:

$$SEL(D') = SEL(D) + LEQ(D') - LEQ(D) + C \log_{10}(D'/D) \quad [Eq 7]$$

and

$$LEQ(D') = 10 \log_{10} \sum_n 10^{[L \frac{1}{3}(n) - \alpha(n)(D'-D)]} - 20 \log_{10} \left(\frac{D'}{D} \right), \quad [Eq 8]$$

where $\alpha(n)$ is the one-third octave attenuation from the Society of Automotive Engineers (SAE) standard 866A⁶ and $L \frac{1}{3}(n)$ are one-third octave levels at D for the maximum 0.5 sec.

Note the difference between Equations 3 and 4 and Equations 7 and 8. Attenuation has been introduced into the calculation of the $LEQ(D)$ for Equations 7 and 8 and the distance factor is now:

$$C \log_{10}(D'/D).$$

Factor C is determined empirically by best fits of lines through distance decay data for a wide variety of aircraft. There is a great amount of scatter among aircraft types as indicated by FAA/USAF data. The USAF has chosen $C = 6.0$ as the best fit whereas the FAA recommends 7.0 dB. The 7.0-dB duration

⁶Standard Values of Atmosphere Absorption as a Function of Temperature and Humidity, ARP 866A (Society of Automotive Engineers, 1975).

factor was used in this report as it gives the best results for the data collected. Variation among aircraft indicates that care should be taken in applying this method--developed for fixed-wing aircraft--to a different class such as the rotary-wing aircraft.

3 DATA ANALYSIS AND COMPARISON WITH FAA PROCEDURE

Data Collection

The helicopter sideline decay data discussed in this report were collected in conjunction with helicopter source data measurements at Fort Campbell, KY. These tests are described in detail elsewhere.⁷ In addition to the source measurement microphones at 61 and 122 m from the centerline, portable recording systems were placed 244, 488, 732, and 976 m from the aircraft centerline (Figure 3). The microphones at 61 and 122 m were B&K 4921 outdoor microphone systems connected to an equipment van. These signals were recorded on an Ampex PR 2230 recorder for later analysis. The additional sideline microphones were B&K 4145 types powered by B&K 2209 Sound Level Meters. The a.c. output of these microphones was recorded on a Nagra DJ set to run at 7.5 ips.

Data Reduction

Data reduction for the 61- and 122-m microphones is described in detail in USA-CERL Technical Report N-131. Data reduction for the sideline tapes was done differently, however. The tapes were played into a system composed of a USA-CERL True-Integrating Environmental Noise Monitor and Sound Exposure Level Meter⁸ and a WANG Model 600 Programmable Calculator. The USA-CERL monitor took buffered 0.5-sec samples of an A-weighted sound pressure level. After the WANG was interfaced to the monitor, it read the data arrays, found the maximum 0.5-sec level and calculated the SEL of the flyby from the 0.5-sec samples.* These levels were then read out on paper tape.

All cases in which the sound flyby did not reach 10 dB down were eliminated. For averaging, only complete sets were used. The 91.5-m flybys at 100 knots were selected for detailed analysis since this minimizes problems with the vertical directivity of the helicopter noise and with signal-to-noise ratios. In addition, the 91.5-m altitude is more typical of helicopter operations on military installations. However, results were also obtained from the 305 m altitude and for different flyby speeds, and these provide some useful information.

Comparative Analysis

Data were averaged for all similar aircraft flybys for which full data sets existed. The first question to be addressed was, "How well does the FAA procedure work in predicting sideline noise decay?" The helicopter spectra developed in USA-CERL Technical Report N-131 were selected for analysis. The

⁷P. D. Schomer, A. Averbuch, and R. Raspet.

⁸P. D. Schomer, A. Averbuch, M. W. Weisberg, R. Brown, and L. M. Little, True-Integrating Environmental Noise Monitor and Sound Exposure Level Meter, USA-CERL TR N-41/ADA060958 (USA-CERL, May 1978).

*Note that this measurement is slightly different from the standard 0.5-sec slow measurement. The difference between the measurements will be small for the slowly varying helicopter sound levels.

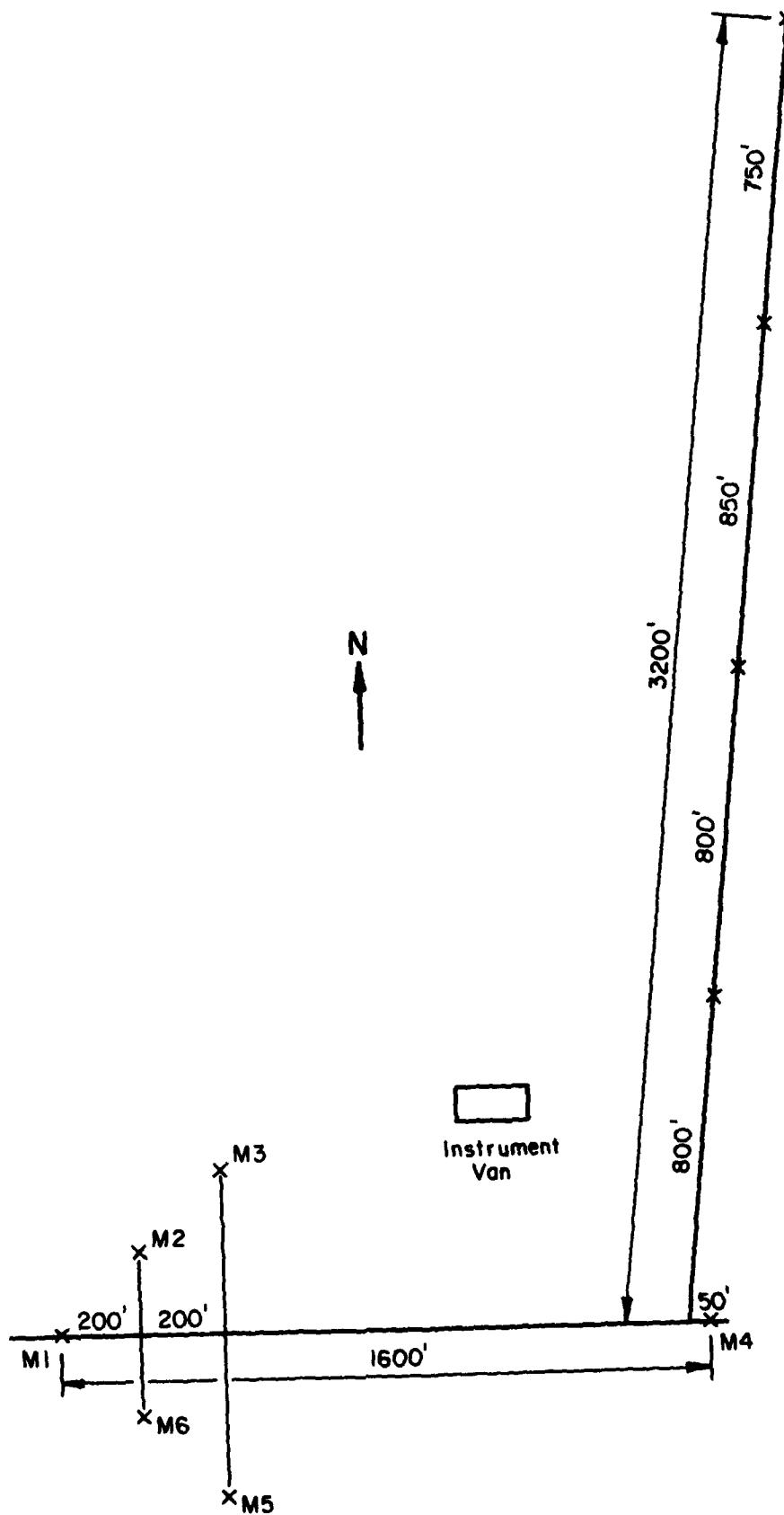


Figure 3. Sideline microphones at Fort Campbell.

spectra for loaded and unloaded UH-60A were very similar, so those from the unloaded helicopter were used to represent both cases with little error.

Figures 4 through 6 display the LEQ and the SEL for the flybys versus slant distance for the three helicopters studied--UH-1H, UH-60A, and CH-47C. These figures are prepared from the average data for 91.5 m AGL and 100-knot airspeed flights. The error bars represent one standard error. The LEQ predicted by the FAA procedure is derived from the source data (correcting the geometrical spreading), from atmospheric attenuation using the SAE standard,⁹ and assuming a hard surface and incoherent sound addition reflection (Equation 8). This prediction is quite accurate up to a 300-m slant distance; beyond this distance, the predicted level is higher than the measured level.

The SEL calculated by Equation 7 begins to deviate from the measured level much more rapidly since it is an integrated level over distances up to three times the slant distance. The predicted level is above the error bars by 300 m slant distance and is 6 to 7 dB above the measured level at 1000 m slant distance.

Figures 4 through 6 also show the results of another calculation. The integral described in Equation 1 has been performed with the level calculated using the SAE standard for atmospheric attenuation. The actual steps in this computer calculation are described in Chapter 4. If only geometrical spreading and atmospheric attenuation are included in a calculation of the flyby SEL, the results are worse than the empirical FAA procedure. The results at 1000 m are about 2 dB greater than with the FAA procedure. In a rough sense, this calculation would correspond to a duration factor of about 9 dB.

Figure 7 plots the average SEL-LEQ versus distance for the three helicopters. The UH-1H displays the closest behavior to the $7 \log (D'/D)$ rule. At short distances, the CH-47C is close to a slope of 7 dB per decade, then levels out. The UH-60A begins with a moderate slope and flattens out. The lines on this figure are fitted to all data points except for those at 738 m since the data points at this distance appear to be systematically low. In addition, the correlation coefficients, r^2 , are low, ranging from .68 to .37.

The relative spectra of the three helicopters were plotted in an attempt to gain some understanding of the flybys' behavior (Figure 8). The spectra shown are normalized to the measured LEQ levels at 110 m slant range and were taken during the maximum 0.5 sec. The UH-1H has a relatively smooth spectra peaking at 315 Hz, the UH-60A has a more narrow high-frequency spectra peaking at 630 Hz, and the CH-47C has a broad spectra with a low-frequency peak at 160 Hz. The CH-47C has much more high-frequency energy above 1250 Hz than either the UH-1H or UH-60A. No strong systematic relationship can be observed between decay rate and spectral type. However, the two lower frequency helicopters displayed decays nearer to 7 dB per decade, whereas the CH-47C, which has more energy at high frequencies, shows a more slowly increasing difference

⁹Standard Values of Atmosphere Absorption as a Function of Temperature and Humidity.

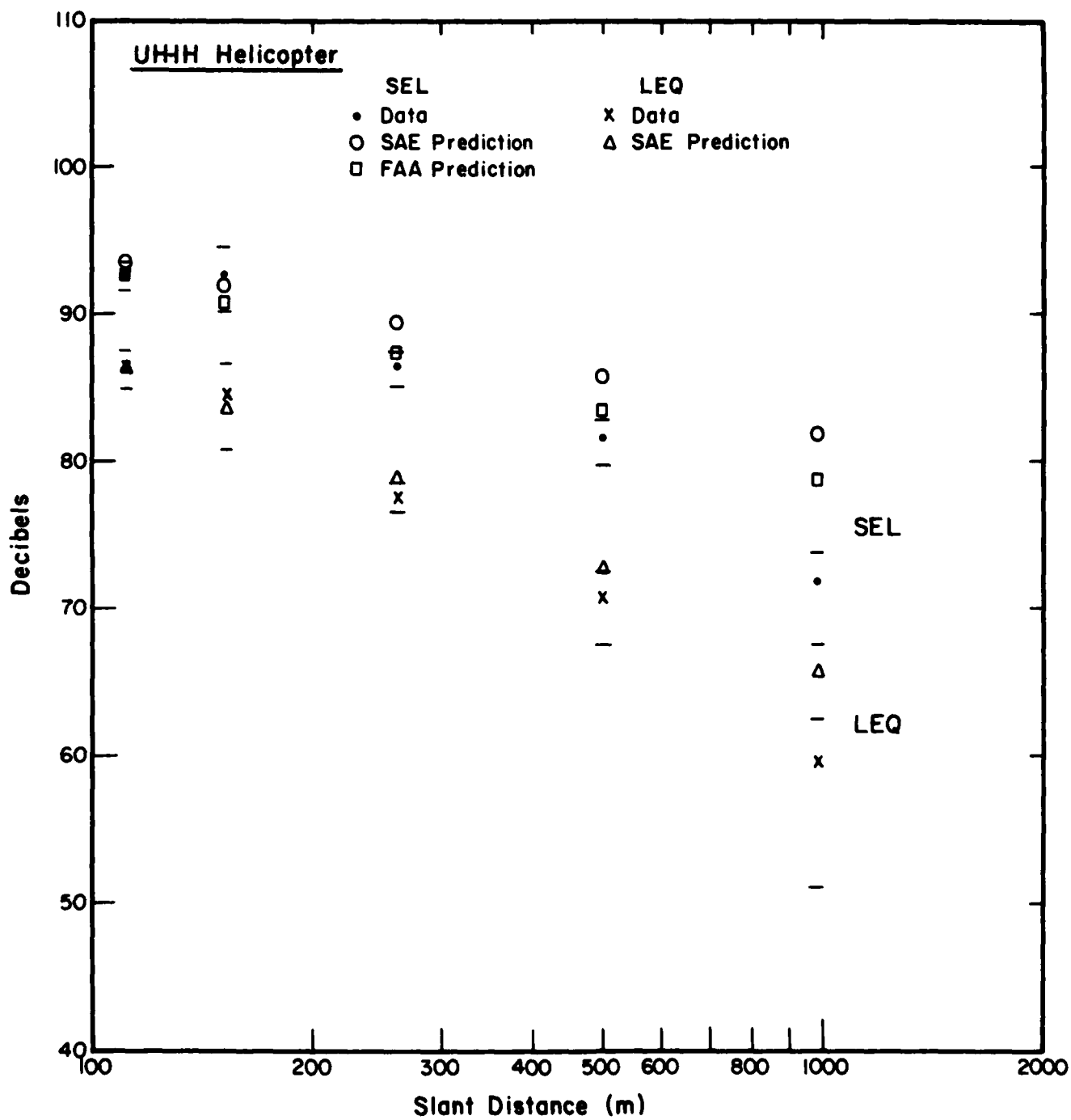


Figure 4. FAA method versus measured levels for UH-1H.

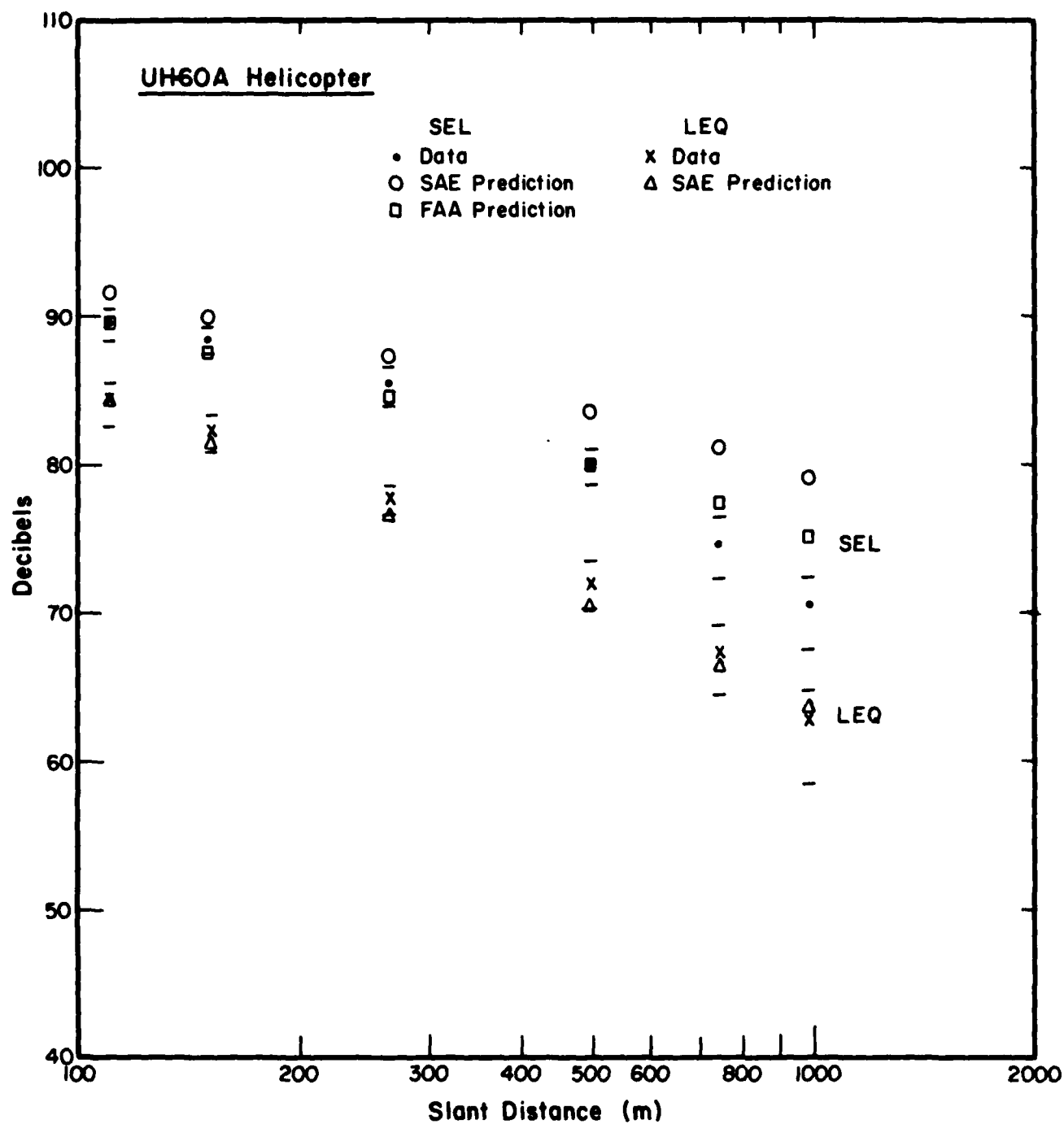


Figure 5. FAA method versus measured levels for UH-60A.

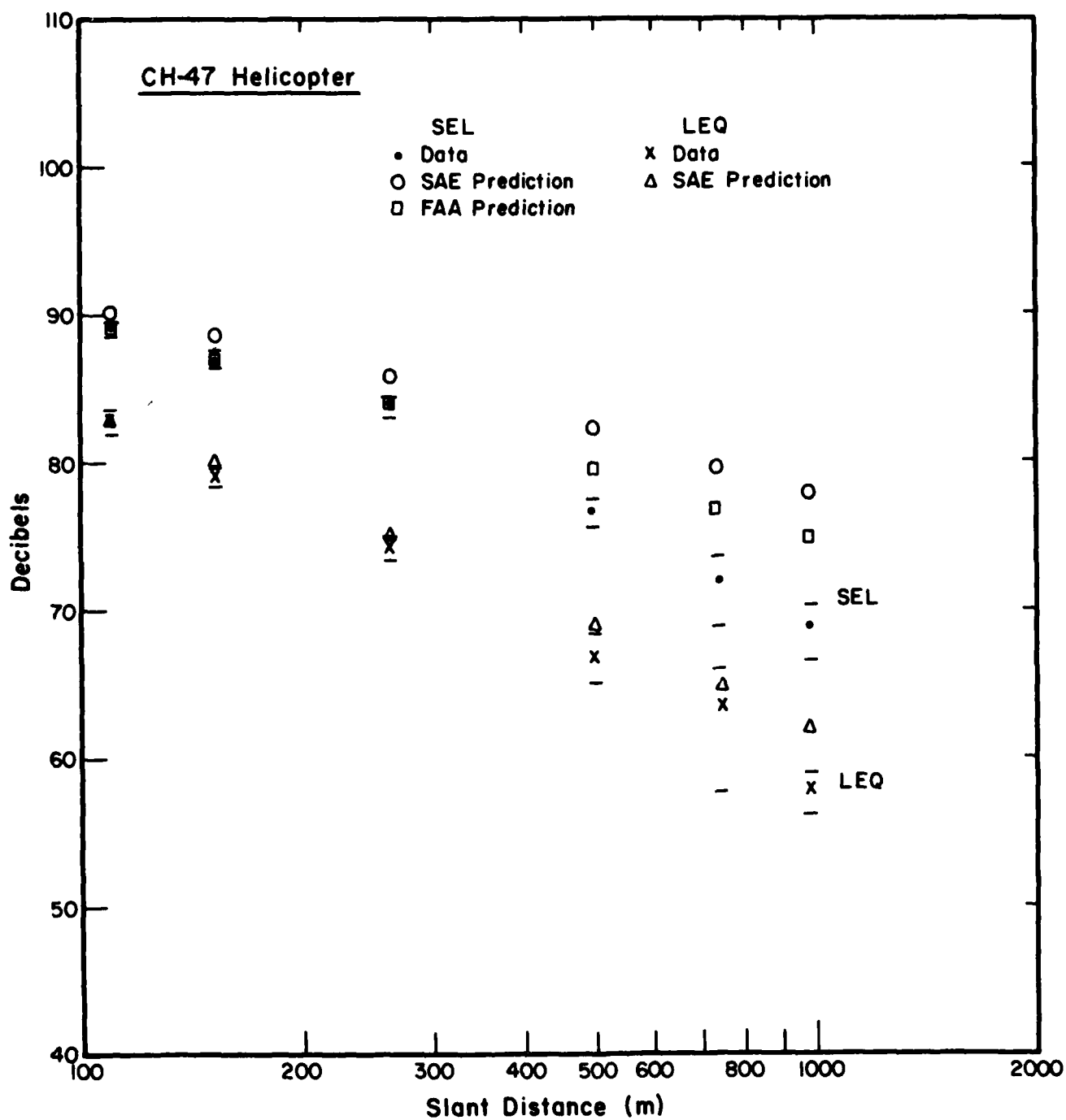


Figure 6. FAA method versus measured levels for CH-47C.

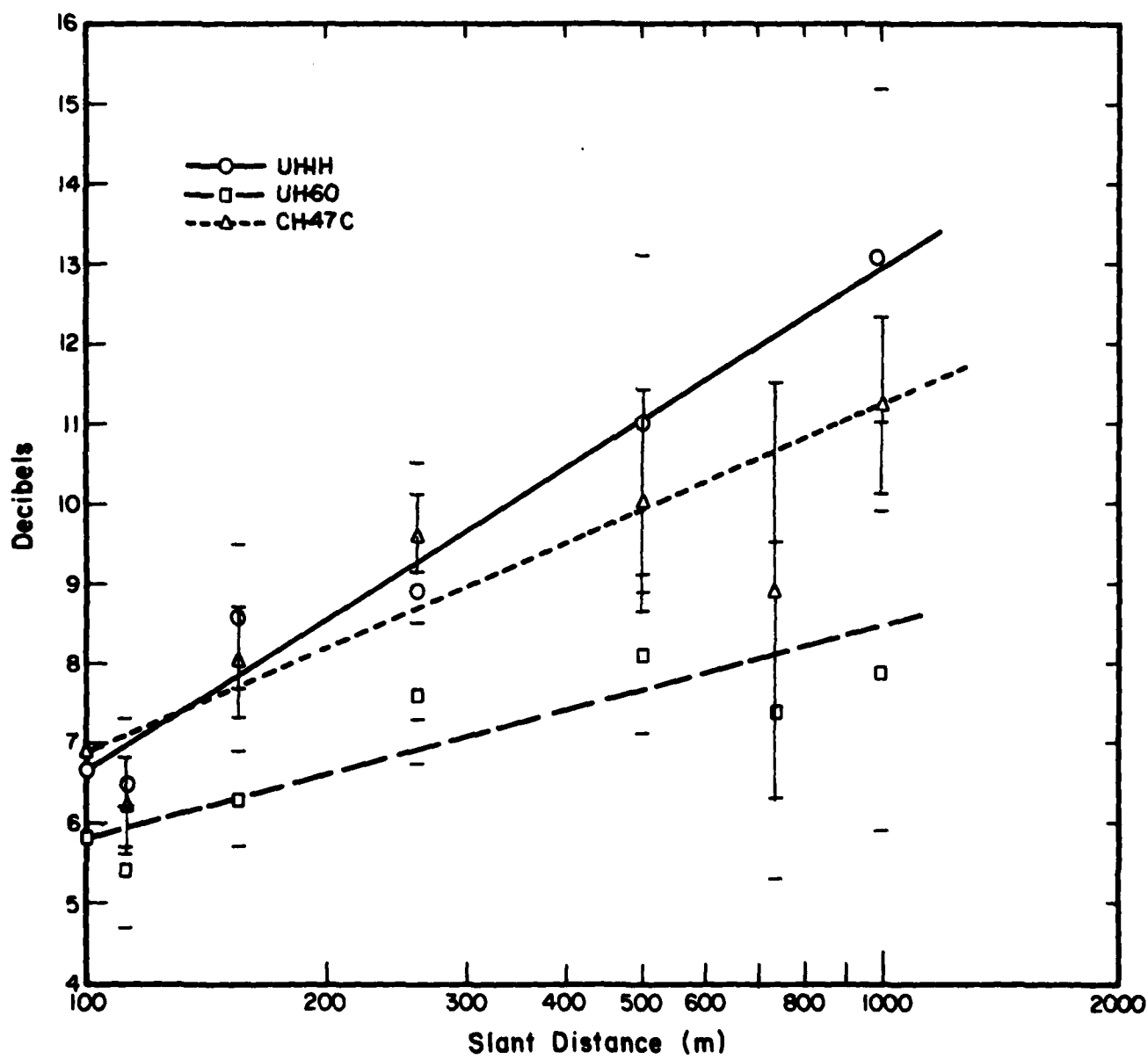


Figure 7. (SEL-LEQ) versus distance.

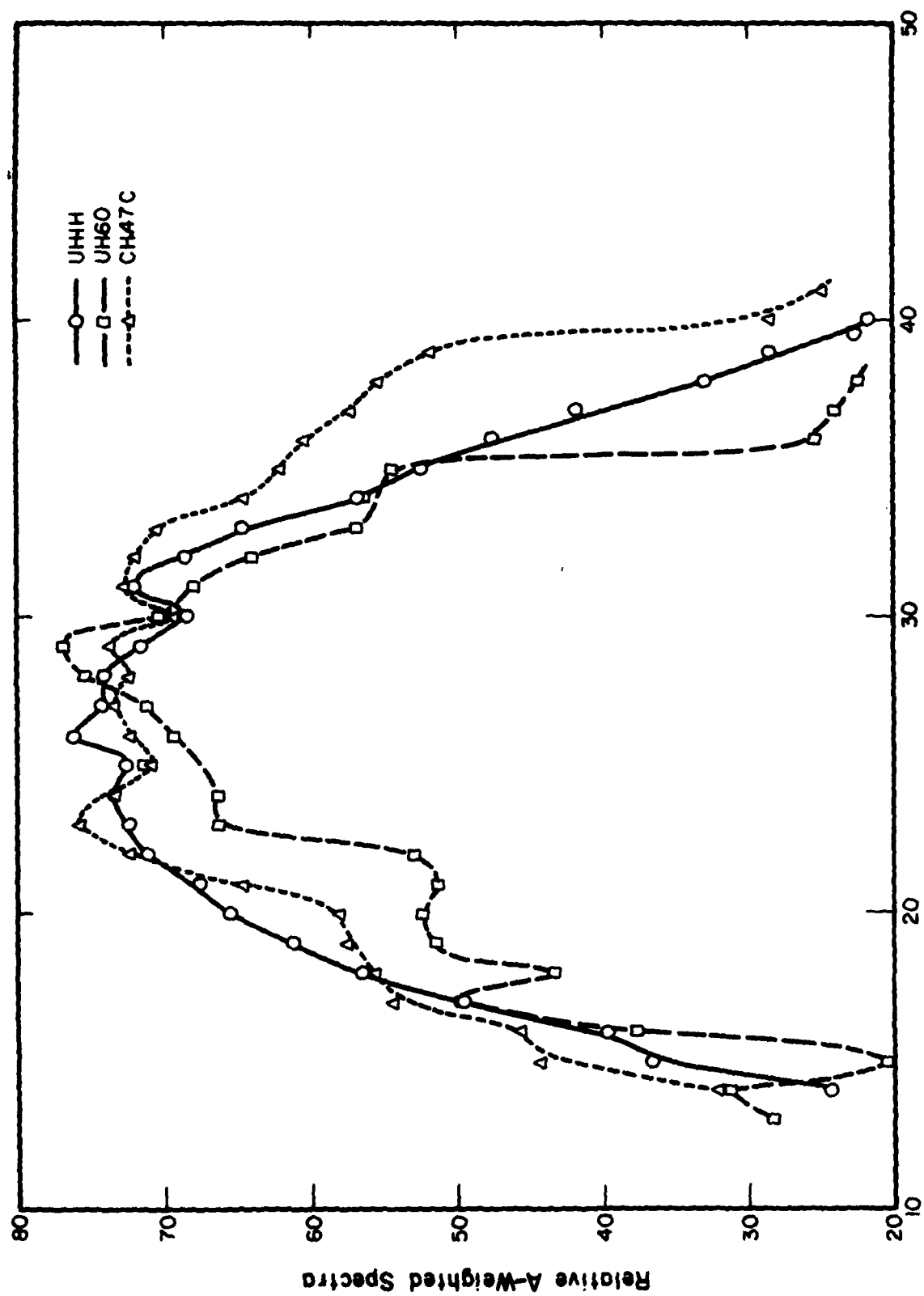


Figure 8. Comparison of normalized A-weighted helicopter spectra.

between SEL and LEQ. The effect of spectral content on decay will be discussed more in Chapter 5.

It was concluded from this analysis that the FAA procedure is acceptable for slant distances up to 300 m. For the CH-47C, the procedure overestimates SEL by 5 dB at 500 m. It is notable that the duration factor's actual behavior varies among helicopters. There is a tendency for the difference between the SEL and LEQ to become almost constant as the distance increases. SEL predictions for the UH-1H, which has an experimental duration factor closest to 7 dB per decade, are no better than predictions for the other helicopters. The measured LEQ in this case is much below the predicted LEQ, so that the measured SEL is also below the predicted SEL.

4 COMPUTER MODEL FOR FLYBY INTEGRATION

Chapter 3 has shown that neither the FAA procedure nor a calculation performing the actual integral and using only SAE attenuation and incoherent addition could adequately describe the sound decay with distance for large slant distances. Therefore, a detailed computer model called "NHELI" was constructed to perform the integration for a flyby. Options included in this model are:

1. Hard or finite impedance¹⁰ ground surface
2. SAE 866A or ANSI S1.26¹¹ atmospheric attenuation
3. Coherent or incoherent interference between the direct and reflected wave. The two extreme cases of completely coherent or completely incoherent were modeled for lack of information on atmospheric stability or instability.

Input for this program is the one-third-octave source spectrum of the helicopter type during the maximum 0.5 sec at a reference distance of 91.5 m. The LEQ for any distance is calculated in this program by three steps:

1. Atmospheric attenuation and spherical spreading are calculated for each one-third-octave band. The A-weighted factor is also introduced at this stage.
2. The ground attenuation relative to 0 dB at 1 m is calculated either with a reflection coefficient of 1 or from Donato's notation for reflection from a finite impedance ground. If coherent addition is specified, the complex amplitudes are added and then multiplied by the complex conjugate of this total to give energy; if incoherent addition is specified, the amplitudes of the direct and reflected waves are each multiplied by their complex conjugates and then added.
3. The factors above are combined to give the one-third-octave level, which is then summed to give the total LEQ.

The LEQ is calculated for the slant distance to begin the integration. Under the assumption of spherical symmetry, the LEQ occurs at the distance of closest approach. This value is stored for later comparison.

¹⁰R. J. Donato, "Propagation of a Spherical Wave Near a Plane Boundary with a Complex Impedance," J. Acoust. Soc. Am., Vol 60, No. 1 (July 1976), pp 34-39. Although Donato's results are used, an improved derivation of the finite ground impedance results can be found in: Keith Attenborough, Sabih I. Hayeh, and James M. Lawther, "Propagation of Sound Above a Porous Half Space," J. Acoust. Soc. Am., Vol 68, No. 5 (November 1980), pp 1493-1501. The results of both theories are very close, however, for geometries and frequencies in this study.

¹¹American National Standard Method for the Calculation of the Absorption of Sound by the Atmosphere, ANSI S1.26 (American National Standards Institute, 1978).

The horizontal ordinate y is incremented by a small step and the SEL for this step is calculated as above. The choice of increment is important: it should be small enough so the phase difference between direct and reflected waves changes slowly for all significant frequencies (A-weighted one-third-octave contribution down 10 dB from the peak). Five hundred steps were found to accommodate all coherent cases. The requirement is not as stringent for incoherent addition and 100 steps were enough. The integration range was chosen to be $3.1 D$ where D is the slant range. The incrementing and calculation were continued until the LEQ for the segment was 10 dB down from the LEQ (D). Figure 9 is a flow chart for this routine and Figure 10 is a typical output.

Since the one-third-octave spectra were relative values, the LEQ at the distance of closest approach 110 m is forced to agree with the data and all other distances are corrected by this same amount when the prediction is compared with actual data.

Attenuation Model

This computer model was used to study the sensitivity of SEL and LEQ to certain known variables. The first step was to compare the SAE 866A standard with the ANSI S1.26 standard for the same atmospheric conditions. Table 1 shows the results for incoherent propagation temperature 15°C, relative humidity 70 percent, helicopter flights at 100 knots, and altitudes of 91.5 m AGL. The differences between the two methods are very minor for the helicopter tested. However, these differences would be significant if individual one-third-octave bands at higher frequencies were examined.

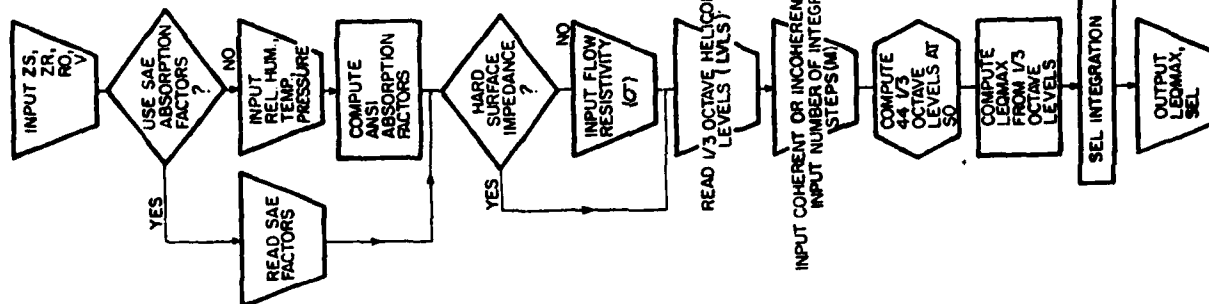
Coherent Versus Incoherent: Hard Surface

Coherent or incoherent addition of the direct and reflected waves from a hard surface was next examined. The strength of this test is limited by the spectral representation in one-third-octave bands rather than in narrow bands; however, for the altitude and slant ranges in this study, the interference bands are quite broad compared to single one-third-octave bands. The helicopter spectra are relatively broadband, so this sensitivity test can still provide useful information. Figures 11 through 13 show results for the three helicopters at a 91.5-m AGL altitude, 1.2-m microphone height, 100-knot aircraft speed, 15°C temperature, 70 percent relative humidity, and 1.01 kPa pressure.

Figures 4 through 6 show incoherent hard surface results for comparison with the FAA method. For all helicopters, the coherent SEL and LEQ are lower for intermediate ranges and slightly higher at long ranges at which the phase difference between direct and reflected rays becomes small. The maximum difference occurs for the UH-60A's LEQ.

The LEQ is expected to be more sensitive than the SEL to whether the direct and reflected waves are coherent or incoherent, since SEL is an integral over many positions whereas the maximum LEQ (LEQMAX) depends on interference at one location. These effects are expected to be greatest for the UH-60A

SOURCE HEIGHT
RECEIVER HEIGHT
HORIZONTAL SEPARATION
VELOCITY
TYPE OF HELICOPTER



(SEE DETAILED CHART)

(SEE DETAILED CHART)

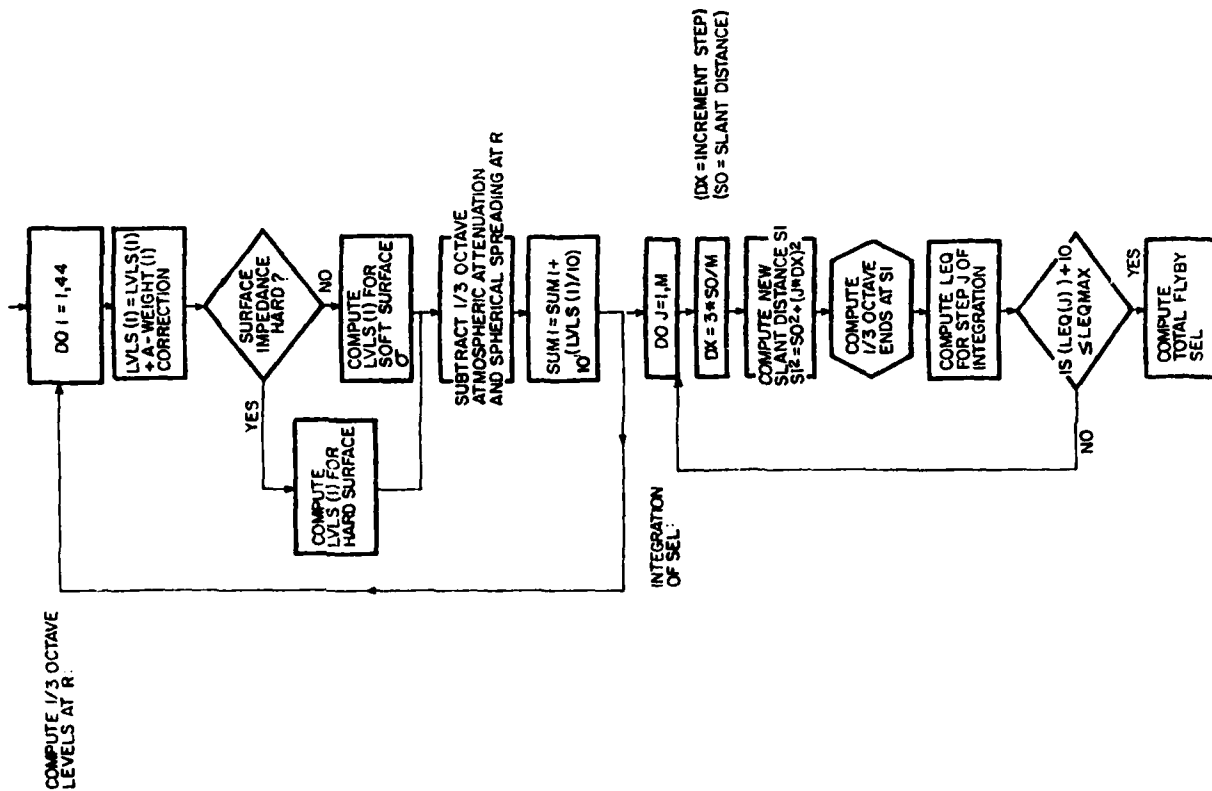


Figure 9. NHELI program flow chart.

ALTITUDE = 91.50 M
 MIC HEIGHT = 1.20 M
 DISTANCE MIC OFF FLIGHT TRACK = 120.00 M
 VELOCITY = 51.400 M/SEC
 USING ANSI ABSORPTION FACTORS (VIA AIR48)
 REL HUMIDITY = 64.0 %
 TEMPERATURE = 300.0 K
 PRESSURE = 1.0 ATM
 SURFACE IS SOFT
 SIGMA = 100.00
 NUMBER OF STEPS TO BE USED FOR INTEGRATION = 100

FOR COHERENT INTERFERENCE ASSUMED...

SO = 150.90
 V = 51.400
 LEQMAX = 76.85
 SEL = 84.67
 TMAX = 14.327

FOR INCOHERENT INTERFERENCE ASSUMED...

SO = 150.90
 V = 51.400
 LEQMAX = 76.61
 SEL = 84.70
 TMAX = 14.797

Figure 10. Sample output of NHELI program.

Table 1

Computer-Calculated Comparison of SAE and ANSI Standards

	Dist. (m)	SAE LEQ	SEL	ANSI Using SAE Std. Cond.	
				LEQ	SEL
UH-1H	110.25	83.82	90.36	83.82	90.36
(NHELI 1)	260.59	75.18	85.88	75.17	85.94
	737.7	66.06	82.05	66.17	82.12
UH-60A	110.25	80.26	87.94	80.26	87.94
(NHELI2)	260.59	71.92	83.19	71.91	83.20
	737.7	59.99	76.89	60.08	76.82
CH-47C	110.25	78.04	84.40	78.05	84.42
(NHELI 4)	260.59	68.87	79.98	68.90	80.09
	737.7	60.13	75.76	60.36	76.03

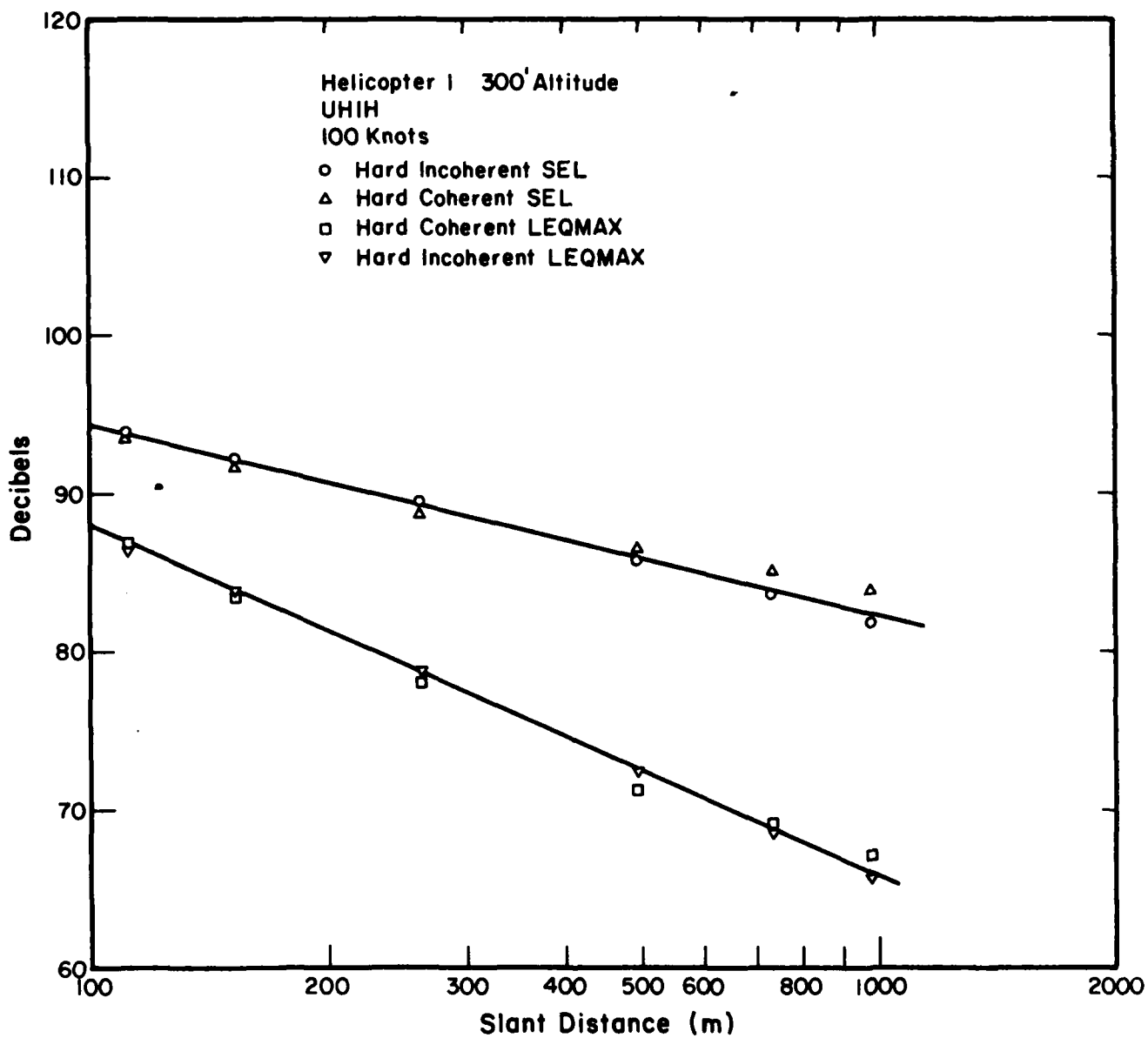


Figure 11. NHELI predictions for US-1H over hard surface.

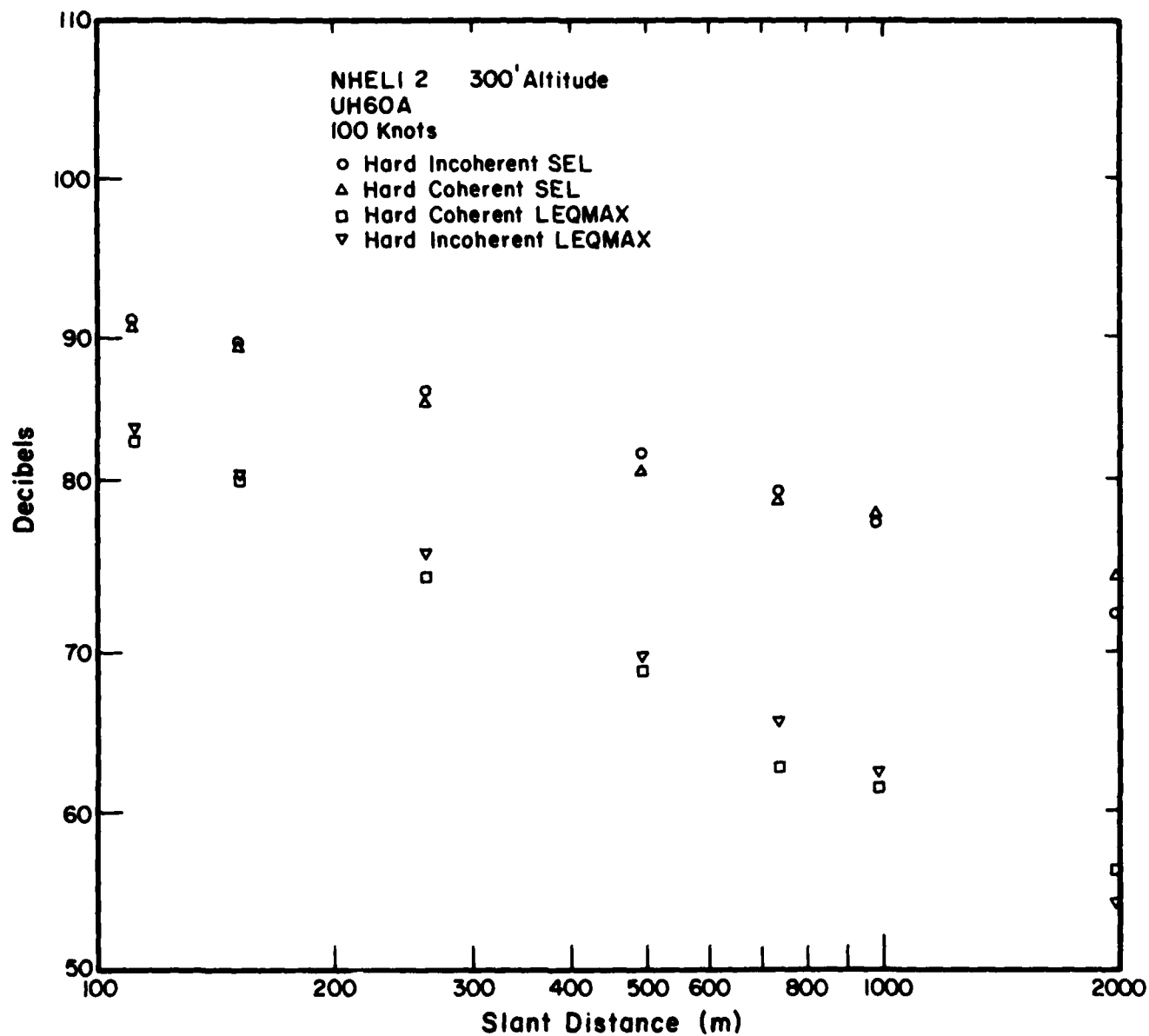


Figure 12. NHELI predictions for UH-60A over hard surface.

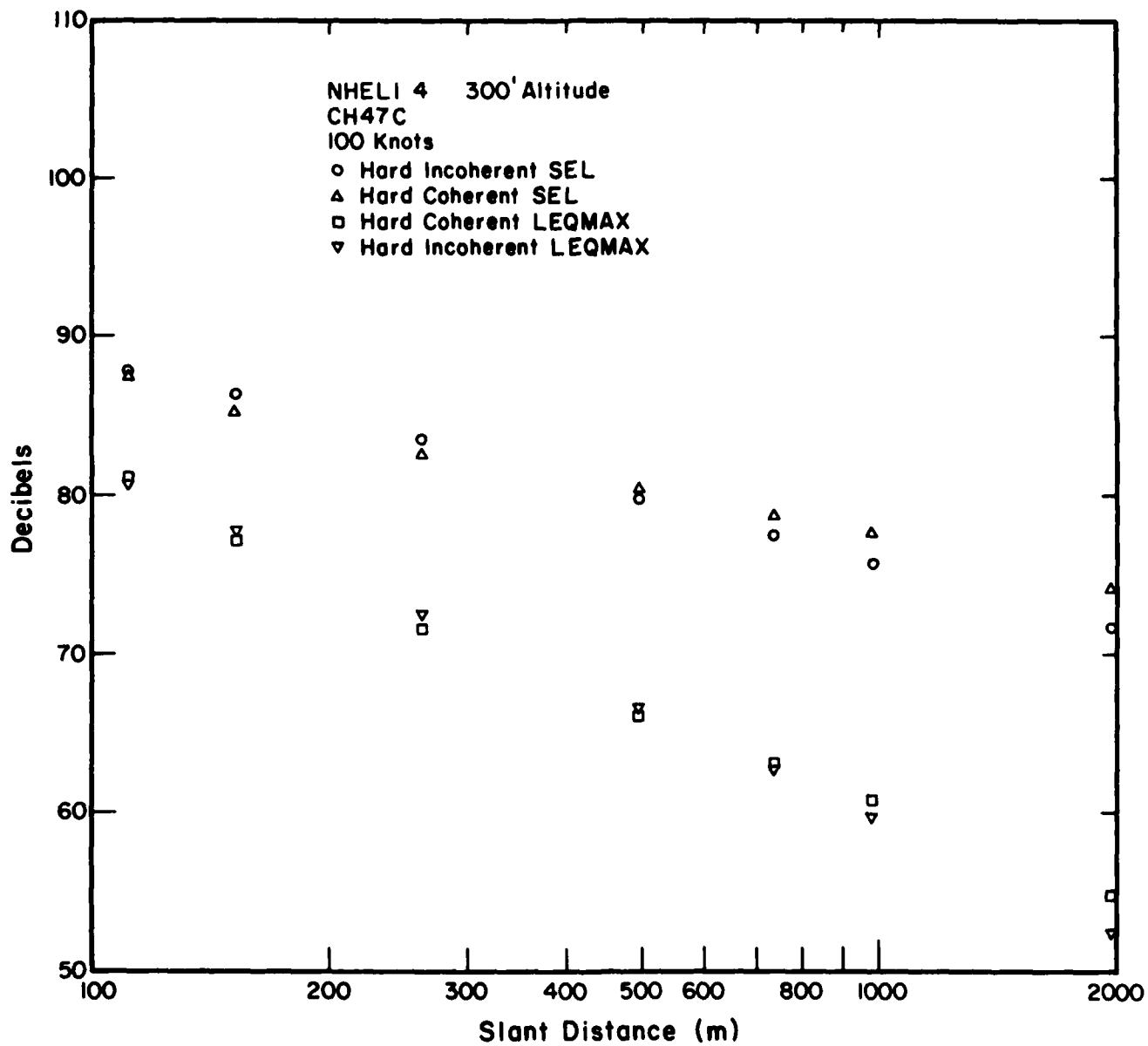


Figure 13. NHELI predictions for CH-47C over hard surface.

because its spectrum peaks sharply at 630 Hz rather than showing wideband behavior like the CH-47C and UH-1H.

Coherent Versus Incoherent: Finite Impedance Surface

Coherent and incoherent propagation above a finite impedance surface were next examined. The porosity was chosen to be 100 (cgs rayls), which is representative of a loose, grassy surface. The other variables are as described in the preceding section.

The finite impedance calculation is the most interesting because it best represents the sideline conditions at Fort Campbell. Comparing Figures 14 through 16 with Figures 11 through 13, the reduction due to the finite impedance ground is quite large; the incoherent SELs are reduced by 3 to 4 dB at 1000 m slant distance, and the coherent ones are reduced even more. The difference between the coherent and incoherent cases above finite impedance ground is 2 to 3 dB. This is expected since, at large slant ranges, much of the spectrum undergoes a phase change near π due to ground reflection near π . At long slant ranges, the direct and reflected path difference is small and cancellation occurs for coherent addition; under the assumption of complete incoherence, intensity addition occurs.

Turbulence was not measured at Fort Campbell, so it is not possible to calculate the mutual coherence as derived by Daigle.¹² However, coherence for ground level propagation can be estimated for a typical day.

From Daigle, the lateral coherence estimated at 3000 m for a 340-Hz signal on a summer day ($\langle \mu^2 \rangle = 10 \times 10^{-6}$) is on the order of 0.5 and, at 1000 m, about 0.8. Since turbulence decreases¹³ rapidly with altitude, the complete coherent calculation should be the more accurate expression for sideline decay. This is an important conclusion even for source measurement, since the microphone height does affect the measured content of the source spectra for coherent conditions.¹⁴

Figures 17 through 19 compare this "best" model with the Fort Campbell measurements. In this comparison, the predicted LEQ has been adjusted to match the measured LEQ. This adjustment is necessary since the source spectra used are relative, not absolute.

The agreement between the finite ground impedance, coherent interference model, and the data is quite good out to 500 m except for the UH-60. For that helicopter, the procedure of aligning measured and predicted LEQs resulted in an overprediction of SEL even at close distances. The SEL's general behavior

¹²G. A. Daigle, J. E. Piercy, and T. F. W. Embleton, "Effects of Atmospheric Turbulence on the Interference of Sound Waves Near the Boundary," J. Acoust. Soc. Am., Vol 64, No. 2 (1978).

¹³E. H. Brown and S. F. Clifford, "On the Attenuation of Sound by Turbulence," J. Acoust. Soc. Am., Vol 60, No. 4 (1976).

¹⁴D. F. Pernet, The Effect of Small Variations in the Height of a Microphone Above Ground Surface on the Measurement of Aircraft Noise, Acoustics Report AC77 (National Physical Laboratory, October 1976).

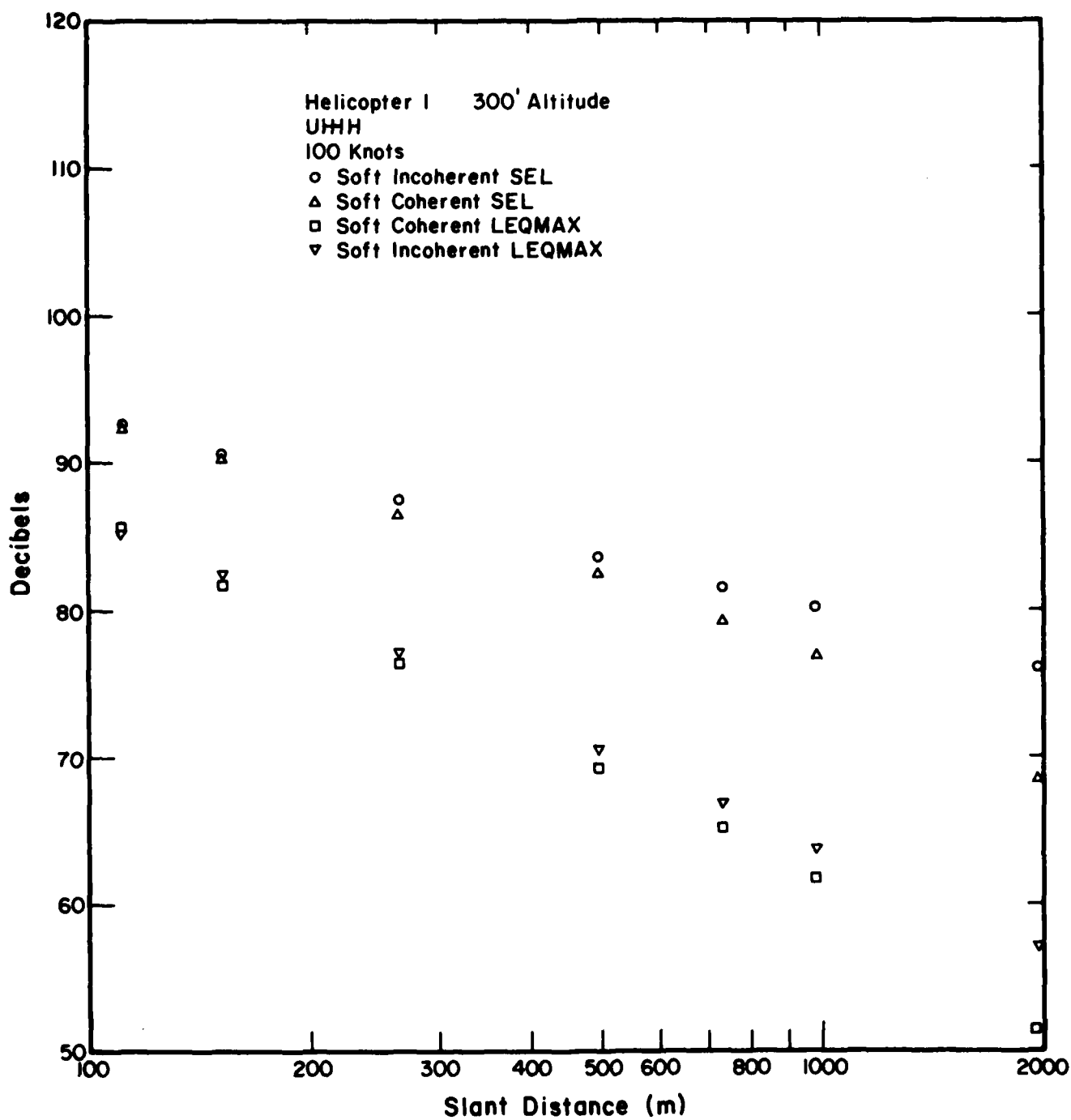


Figure 14. NHELI predictions for UH-1H over soft surface.

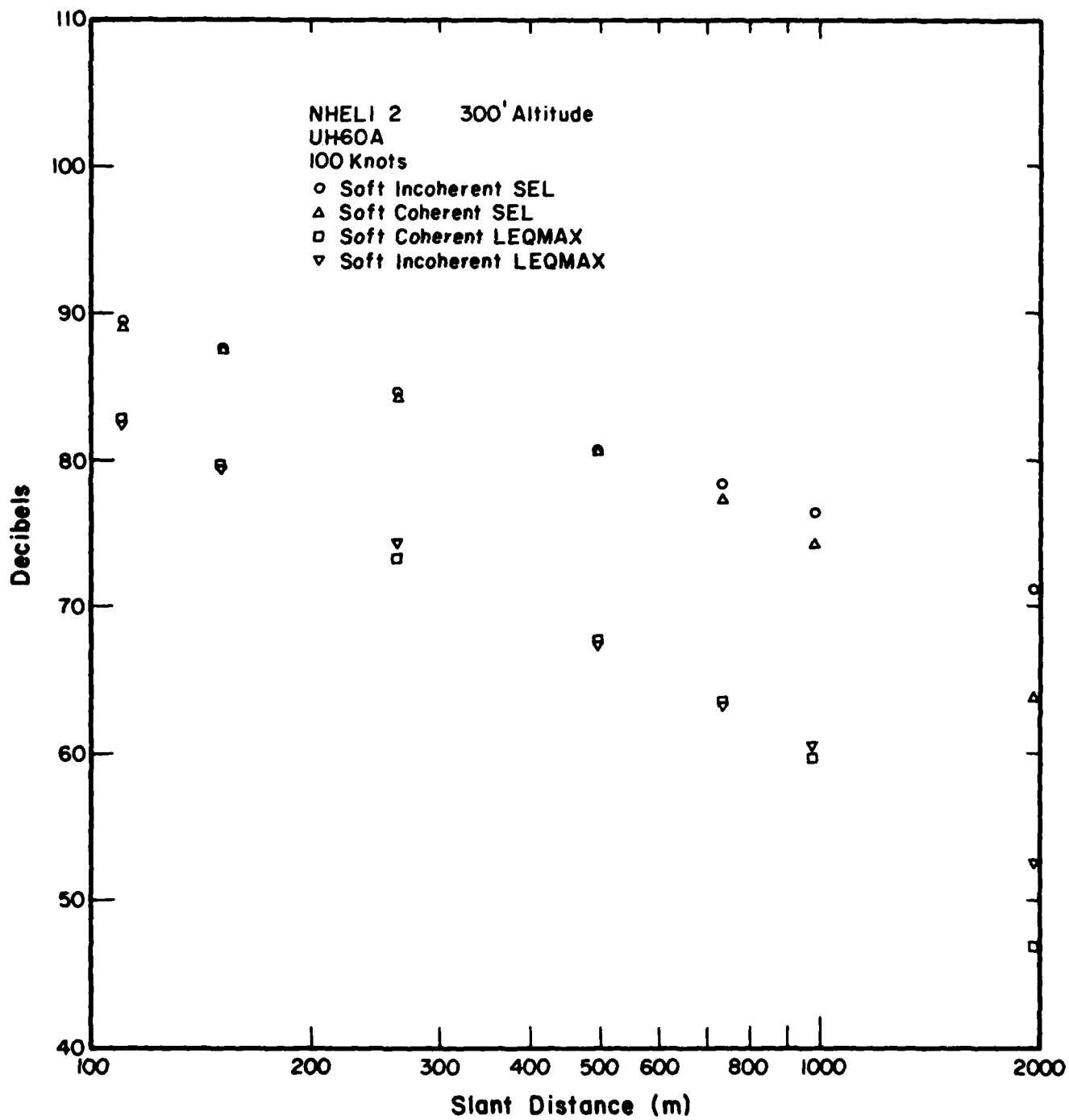


Figure 15. NHELI predictions for UH-60A over soft surface.

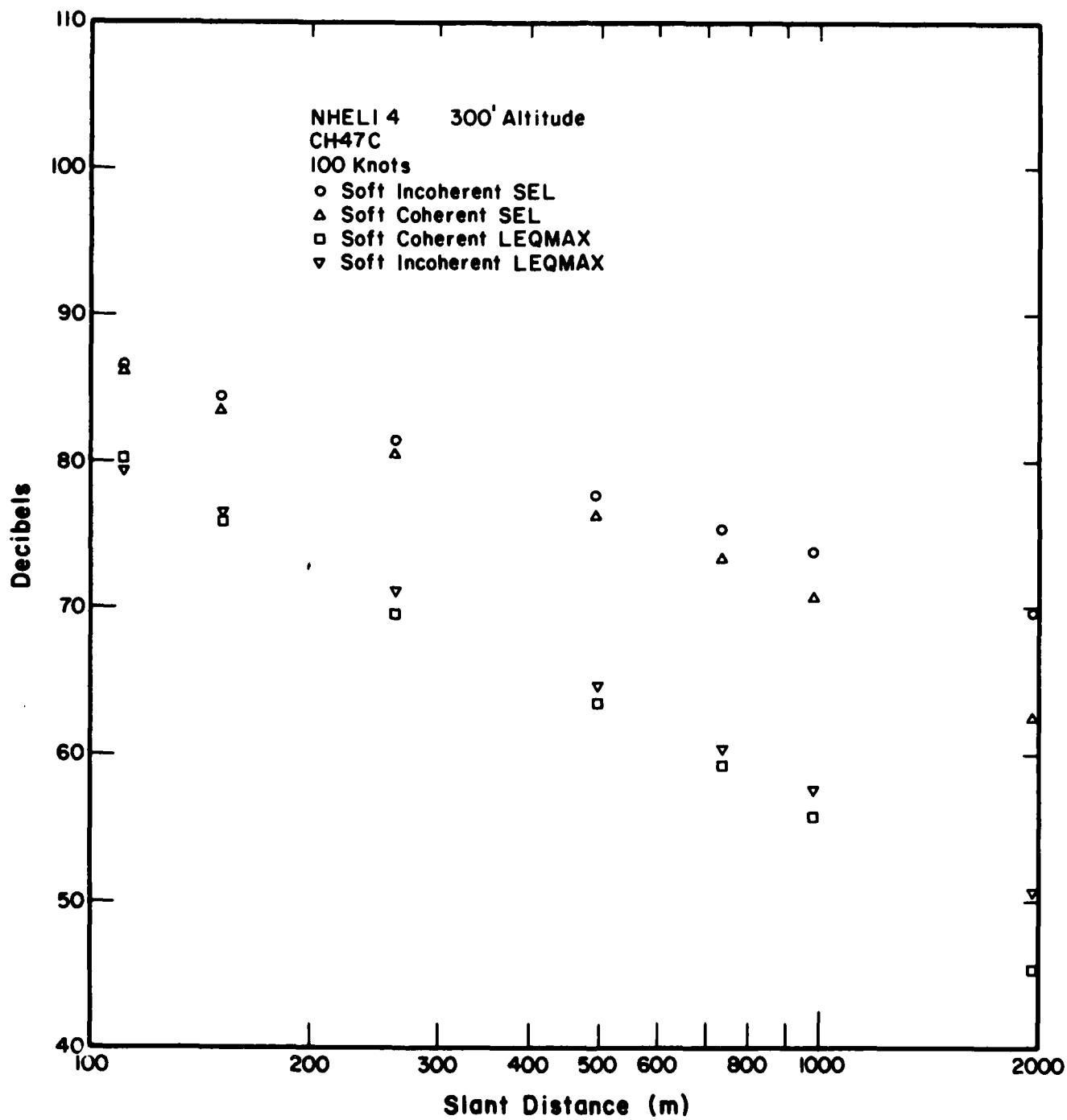


Figure 16. NHELI predictions for CH-47C over soft surface.

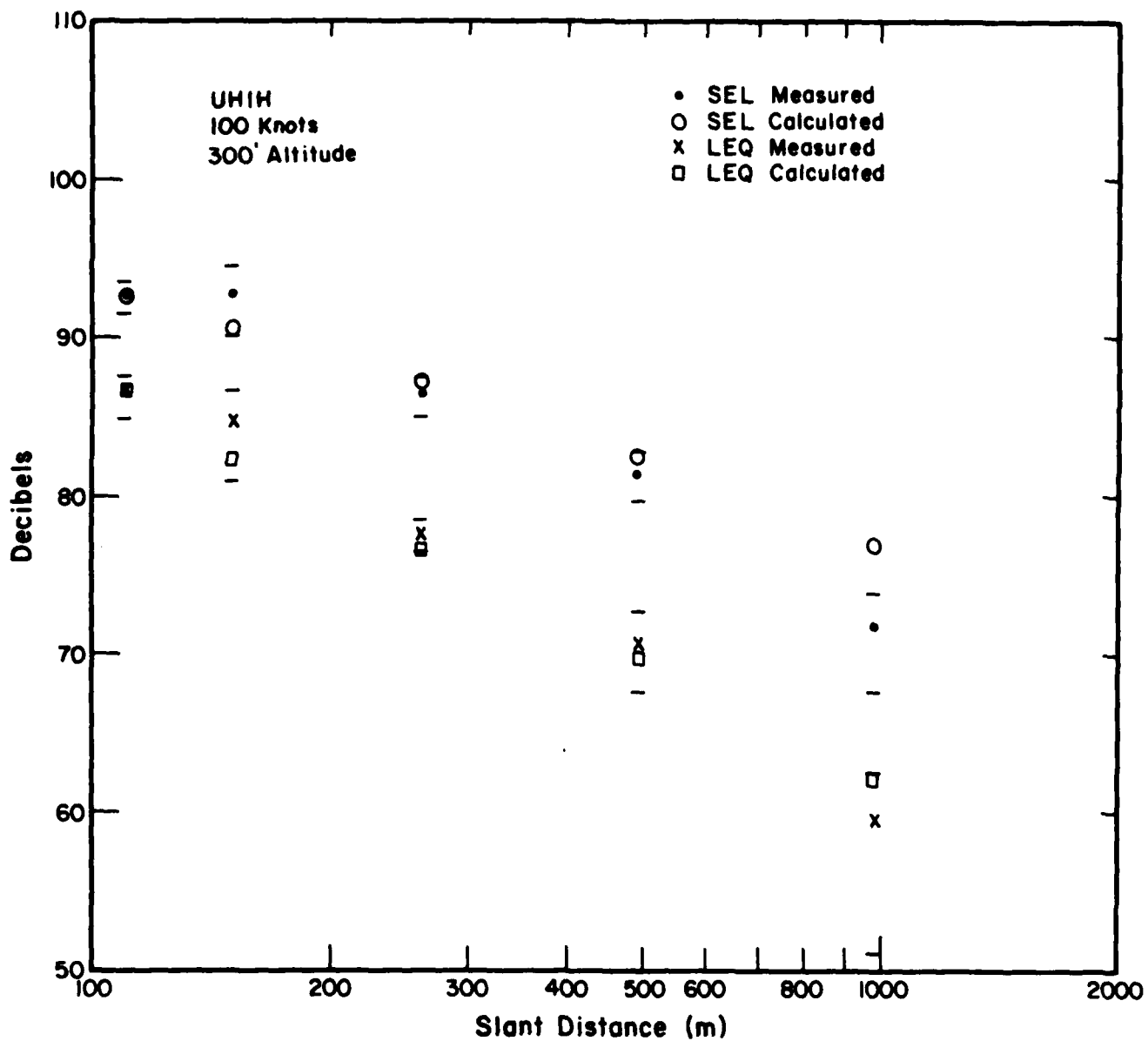


Figure 17. Soft coherent prediction versus measured levels for UH-1H.

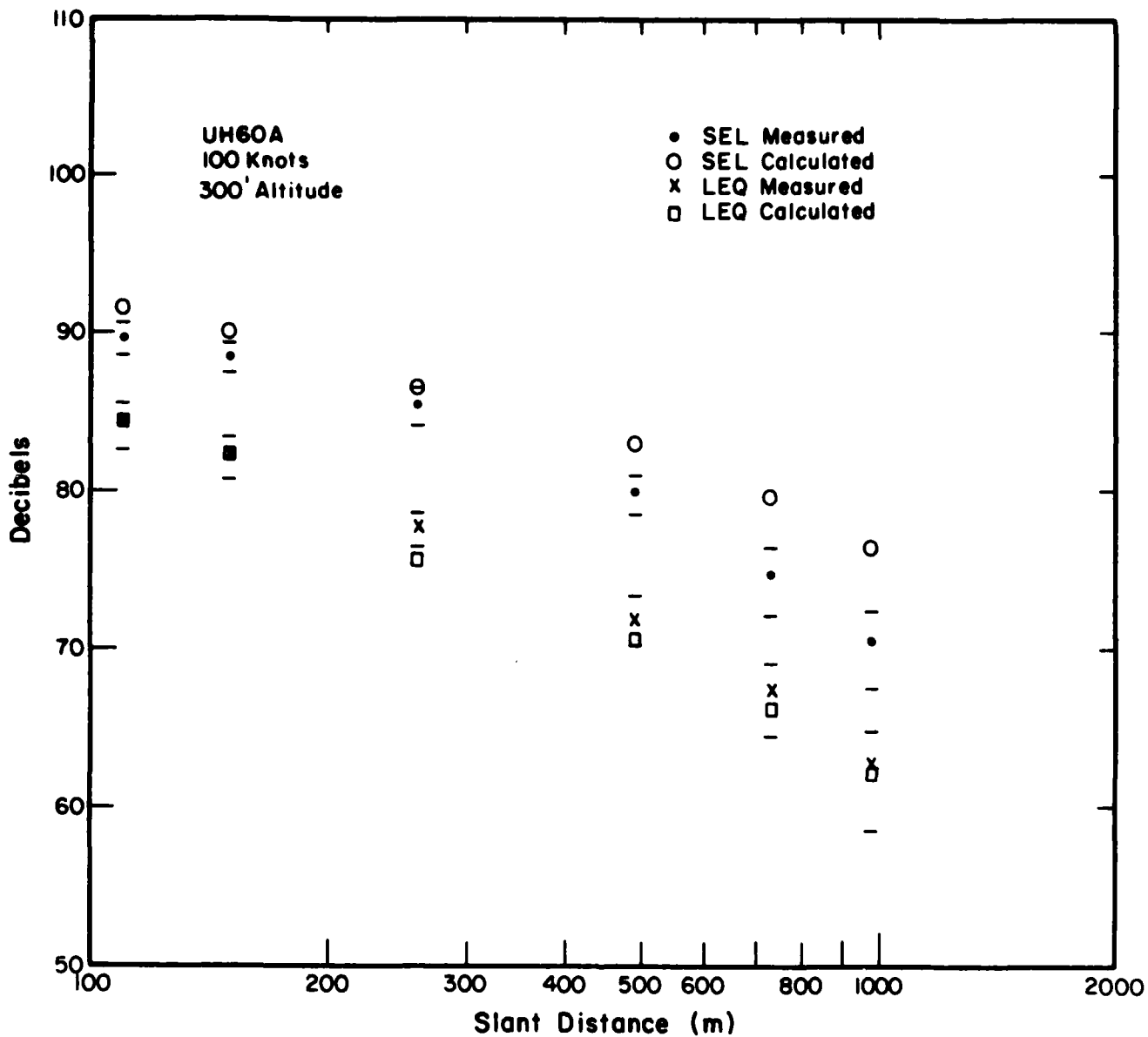


Figure 18. Soft coherent prediction versus measured levels for UH-60A.

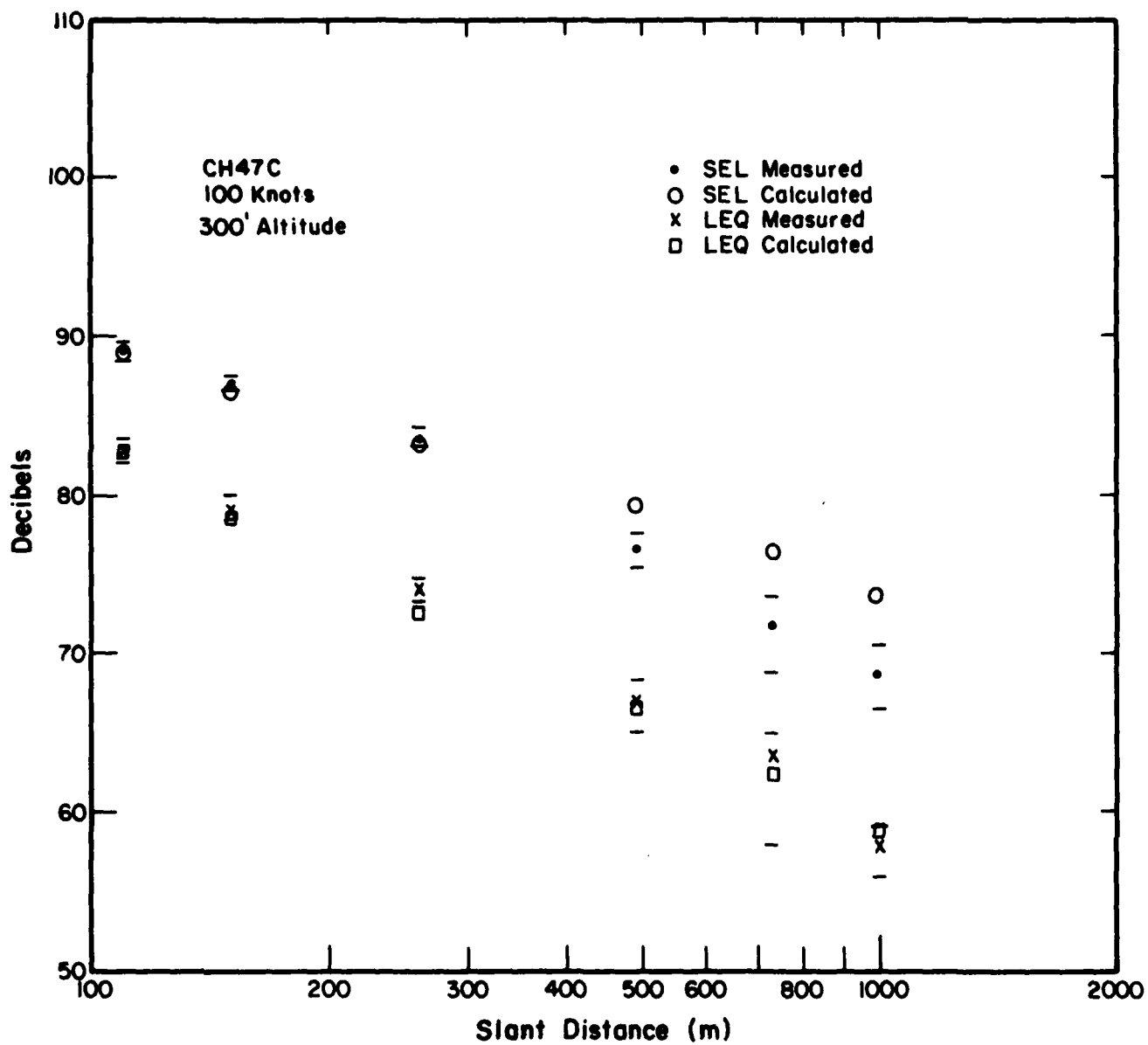


Figure 19. Soft coherent prediction versus measured levels for CH-47C.

is correct, but is about 2 dB high. If the SEL measured at 110 m slant distance is used as the reference point as in the FAA procedure, the prediction is within error bars to 500 m slant distance and above the error bars by less than 2 dB at 730 and 980 m slant distances.

The overestimation of the difference in LEQ and SEL may have resulted from representing the spectra as one-third-octaves rather than as narrow band spectra. For the UH-60A, there is a significant energy peak in the 630-Hz band and constructive or destructive interference for this one frequency greatly affects the calculation. The LEQ was predicted for sideline distances of 70, 80, 90, and 100 m and was found to vary rapidly with a variation of a few dB magnitude. This variation shows the need to consider coherent interference of the direct and reflected paths when the source has pure tones or a sharply peaked spectrum.

Calculation for 305-m Altitude

Sideline decay was calculated using the FAA procedure and the soft coherent integration was performed for UH-1H overflights at a 305-m altitude. Figure 20 shows the results of this calculation. In this case, the measurements were normalized to the 328-m slant range since the vertical directivity pattern has such a large effect on the reading at 310 m slant distance.

The vertical pattern of the rotor noise is discussed in USA-CERL Technical Report N-131. The FAA data are adjusted to give the measured SEL value at 328 m and the integration procedure is adjusted to give the correct LEQ at that slant distance. In this case, the FAA procedure agrees closely with the integration at all points, but both differ from the measured average by 4 dB or more beyond 600 m slant range.

The agreement between the methods at 305 m AGL contrasted with the differences for lower altitude flights demonstrates the importance of finite ground impedance in low-level flight sound prediction. Both procedures overestimated the SEL beyond 600 m.

Variation in Decay Rate With Aircraft Speed

Since the spectra used in the calculations are averaged over many speeds, UH-1H data from the high and low aircraft speeds (40 and 120 knots) were averaged and compared to the 100-knot data. To compare the sound decay, the data were corrected so that the LEQs at 110 m were identical and a speed correction of $10 \log (V/100)$ was added to the SEL data. Figure 21 shows the results along with the calculated levels. The differences in data from the different speeds are random and minor: there is no systematic variation with speed. This does not imply that the noise level stays unchanged with velocity, only that the decay with distance is the same once the data are corrected for velocity and source level.

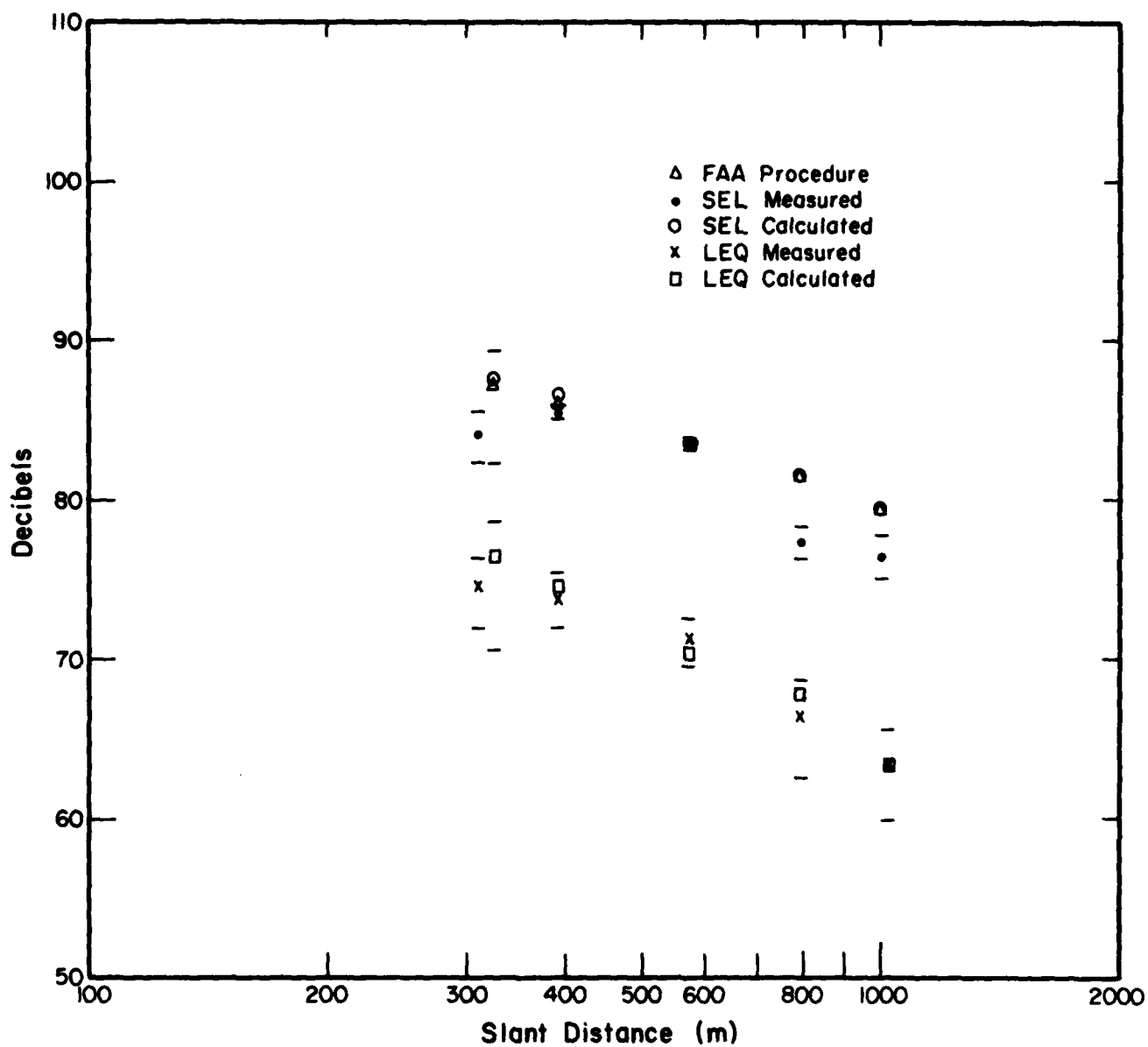


Figure 20. Soft coherent prediction versus measured levels for UH-1H and normalized to 1075.4-ft (328-m) data.

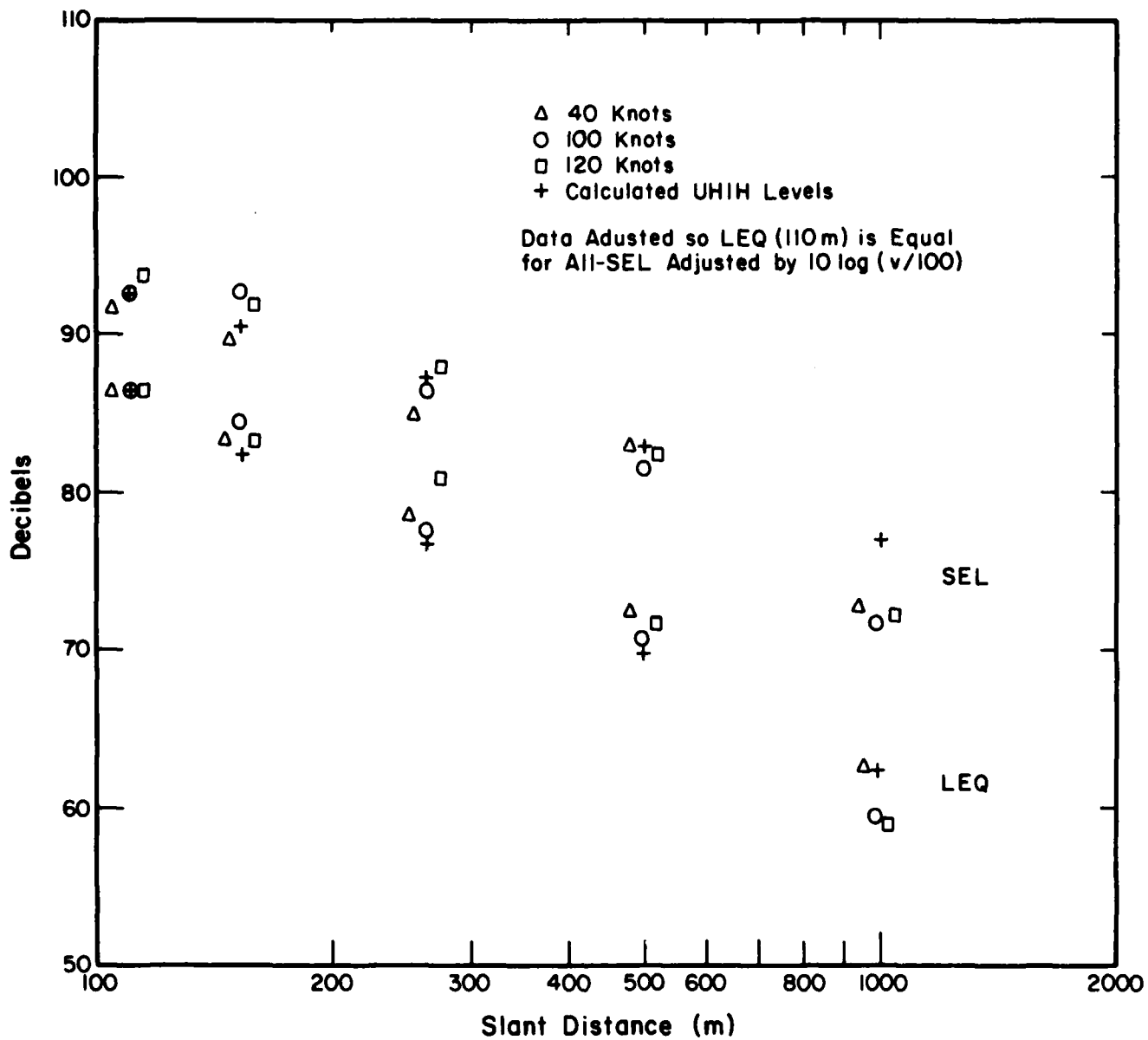


Figure 21. Check for variation in decay with speed.

5 DIRECTIVITY EFFECTS

The model for helicopter sideline noise decay does not allow adjustments for the helicopter directivity pattern or for the change in spectral content as the helicopter is approaching or receding. These two effects were investigated to see if one or both could lead to the excess decay measured at large slant distances.

Effect of Spectral Change on SEL Calculation

The spectral plots in Figure 22 show the change in frequency from mostly low frequencies as the helicopter approaches to mostly higher frequencies as it recedes. These plots are for 0.5-sec spectra of a single UH-1H flyover at

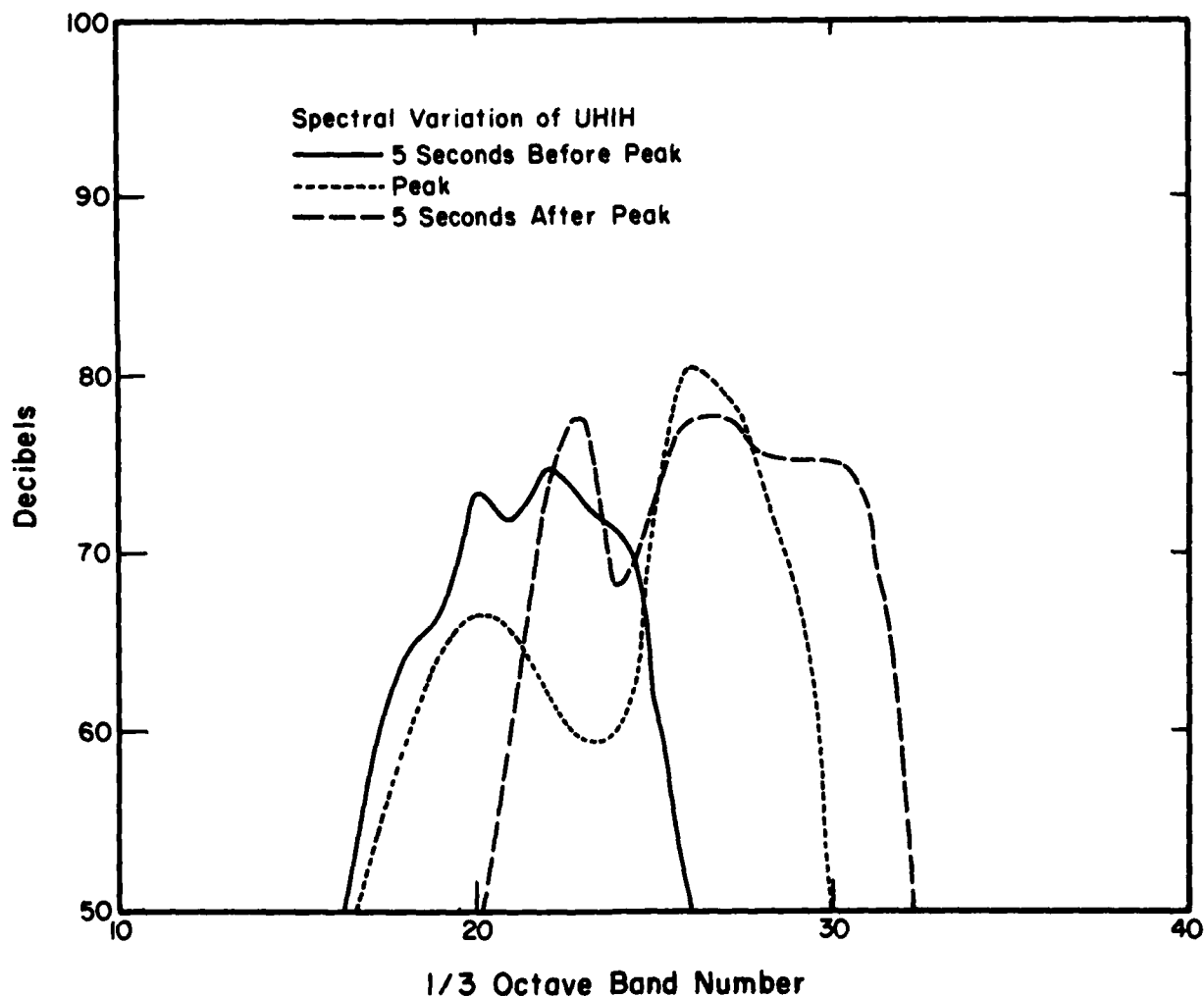


Figure 22. Spectral variation of UH-1H over flyby.

100 knots, 91.5 m altitude, and 122 m sideline distance. The spectra are more irregular than those in Figure 7 since they are not averages. The spectra were taken 5 sec before the maximum 0.5-sec LEQ, at the maximum LEQ point, and 5 sec after the 0.5-sec LEQ. These spectra were corrected for distance. SEL was calculated using the early spectra for the first half of the SEL integration and the late spectra for the second half. The peak spectrum was used to calculate the LEQ at each distance. Figure 23 compares the measured SEL and LEQ to the results of the SEL calculation using the average UH-1H data and the SEL calculated using the early and late spectra. There is no significant difference between the two calculations. Therefore, the difference between calculation and measurement is still significant--5 dB or more at large slant ranges. It is notable that the large asymmetry denoted by the spectra does not affect the SEL calculation for these measurements.

Analysis of Directivity Effects on a Level Flyby

The neutral result from the early-late simulation suggested that directionality effects for ideal cases should be examined. As discussed in USA-CERL TR N-131, vertical directivity can greatly affect microphone levels for near overhead flybys (this has been discussed in Chapter 4 when the 300-m altitude sideline decay was examined). For larger sideline distances and lower altitudes, this effect is smaller since the vertical emission angle varies only slightly with sideline distance, but it is at these larger ranges that the prediction fails. The effects of the changing spectral content due to direction changes were modeled in the preceding section. It can also be demonstrated that any horizontal directivity will not affect the ideal decay rate (the no-attenuation case).

If the pressure is modeled as depending on horizontal direction:

$$p = \frac{P_{\text{ref}} R_{\text{ref}} f(\theta)}{R}, \quad [\text{Eq 9}]$$

where $f(\theta) = 1$ at the direction of maximum emission and R is the distance to the receiver. First, the ideal LEQ is shown to vary as $20 \log d$, where d is the slant distance (Figure 2):

$$P(Y, \theta) = P_{\text{ref}} R_{\text{ref}} \frac{f(\theta)}{\sqrt{d^2 + y^2}}. \quad [\text{Eq 10}]$$

To maximize P for any d , it is expressed in terms of θ only:

$$P(D, \theta) = P_{\text{ref}} R_{\text{ref}} \frac{f(\theta) \sin \theta}{d}. \quad [\text{Eq 11}]$$

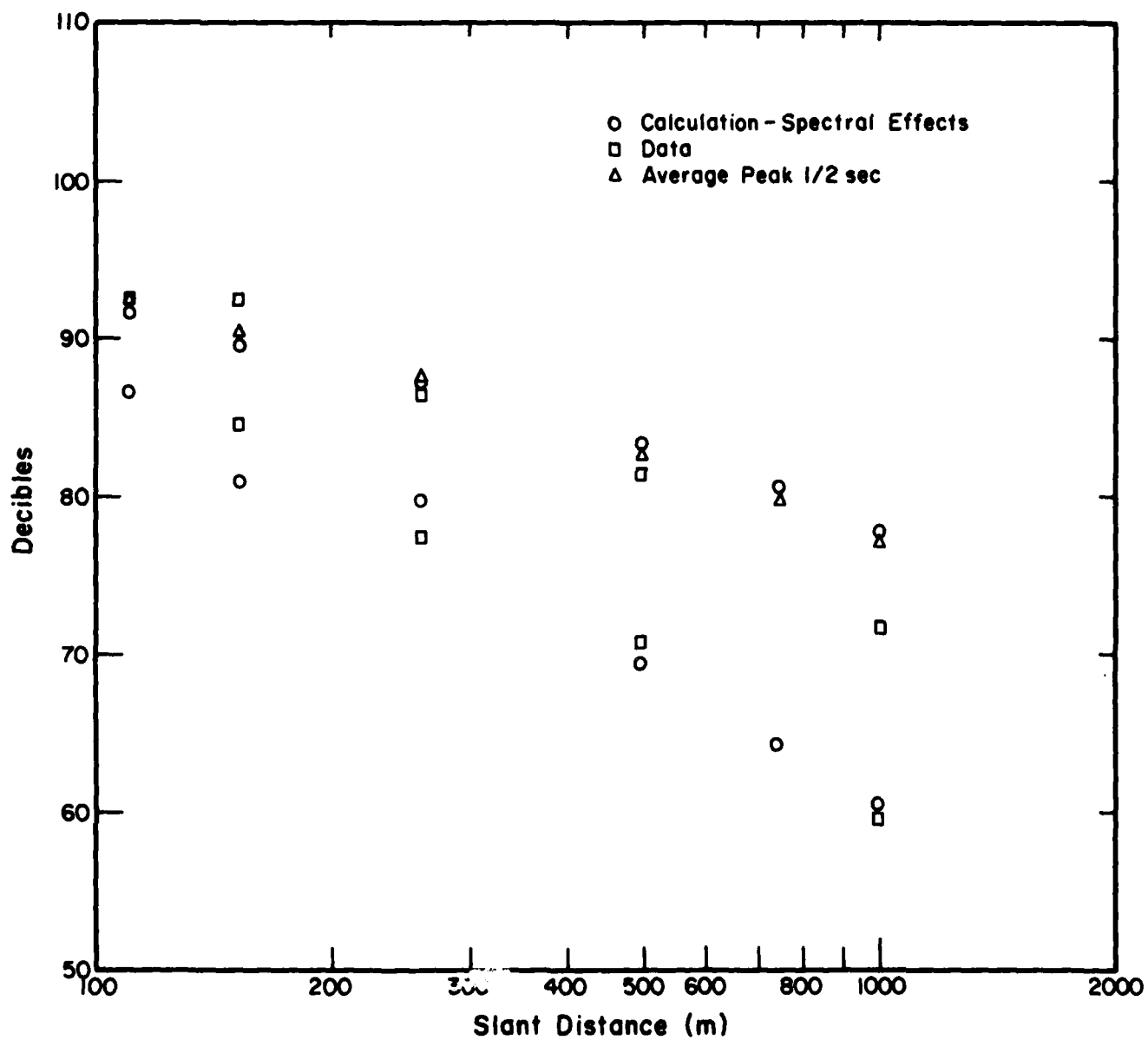


Figure 23. Spectral effects calculation.

The maximum sound pressure level for any slant distance D will occur at the same angle θ such that $f(\theta) \sin\theta$ is a maximum. This implies that:

$$P_{\max} \propto 1/D \text{ and}$$

$$LEQ \propto -20 \log D.$$

Since the pressure level has the angular dependence described in Equation 11, the endpoints (10 dB down points) are also defined uniquely and occur at the same θ_E and θ_L (although the two angles are not necessarily equal). The SEL integral is:

$$I = \int_{\theta_E}^{\theta_L} \frac{P_{\text{ref}}^2 R_{\text{ref}}^2 f^2(\theta)}{D^2 + Y^2} \frac{dy}{v}.$$

$$Y = \frac{d}{\tan\theta} ; dy = \frac{d d\theta}{\sin^2\theta} ;$$

$$D^2 + Y^2 = D^2/\sin\theta.$$

Substituting, the integral becomes:

$$\begin{aligned} I &= P_{\text{ref}}^2 R_{\text{ref}}^2 \int_{\theta_E}^{\theta_L} f^2(\theta) \frac{\sin^2\theta}{d^2} \frac{d}{\sin^2\theta} d\theta \\ &= \frac{P_{\text{ref}}^2 R_{\text{ref}}^2}{D} \int_{\theta_E}^{\theta_L} f^2(\theta) d\theta. \end{aligned}$$

So the pressure squared integral is proportional to $1/D$ and decays as $-10 \log(D)$. This implies that the difference between LEQ and SEL decays as $10 \log(D)$. Note that the directivity can affect the initial values of SEL and LEQ and the relationship between them, but it does not affect the decay rate or the duration factor.

6 FLYBY PROFILES

The excess reduction in SEL with distance indicates there may be an unidentified mechanism for attenuation. To investigate this possibility, the flybys' sound level profiles were examined. This was done by playing the recording into a Bruel and Kjaer Type 2209 sound level meter as the input to a NORLAND 2001 programmable oscilloscope. The output was plotted on an X-Y recorder for the cases shown in Figure 24. Data were also taken using a tunable filter to record the change in level for frequency bands.

The most striking feature of these profiles is the tremendous variation in sound level with time. Much of the variation is due to changes in source level as the helicopter flies through turbulence.¹⁵ However, investigations of this variation as distance increased showed it to be much larger for the far distances (Figure 24). The time between peaks is random but appears to vary on a scale of 5 to 10 sec. Figure 25 presents a flyby profile resolved into frequency bands. The peaks are observable across these bands, which indicates the variations may be due to refraction rather than scattering.

During daytime measurements, it is common to observe high rates of temperature lapse near the ground. The temperature gradient usually varies logarithmically with height; Figure 26 shows data taken between 1115 and 1130 on 30 April 1983 at Bondville Field Station south of Champaign, IL. Although no weather data were taken at Fort Campbell, those taken at Fort Carson, CO, in conjunction with another type of measurement showed significant lapse rates. Figure 27 shows a typical logarithmically varying temperature lapse rate for 4 August 1982 at 1400. Figure 28 gives the associated sound speed lapse. Using a simple three-layer refractive model and a source height of 91.5 m, the intensity was calculated using a simplification of the technique described by Hayes, Haefeli, and Karlsrud.¹⁶ The refractive effects of the temperature gradient produces sound level attenuation and a shadow zone at 1500 m (Figure 29). Unlike a single gradient layer, the three-layer model produces a reduction in intensity with distance compared to a homogeneous, isovelocity atmosphere before the shadow zone forms. More importantly, the upward refraction reduces the apparent source height (Figure 30) and therefore decreases the grazing angle (Figure 31). On a finite-impedance surface, the reduced angle of incidence causes greater surface attenuation.

Fluctuations in the observed flybys could be produced as thermal plumes break away from the ground and move into the region between the aircraft and the microphone.¹⁷ This would produce slow variations in level, with the level dropping as the smoothest profile is reestablished. However, lacking detailed

¹⁵Robert W. Paterson and Roy U. Amiet, Noise of A Model Helicopter Rotor Due to Ingestion of Turbulence, NASA Contractor Report 3213 (National Aeronautics and Space Administration, 1979).

¹⁶Wallace D. Hayes, Rudolf C. Haefeli, and H. E. Karlsrud, Sonic Boom Propagation in a Stratified Atmosphere, With Computer Program, NASA Contractor Report CR-1299 (National Aeronautics and Space Administration, 1969).

¹⁷S. David Roth, Acoustic Propagation in the Surface Layer Under Convectively Unstable Conditions, Ph.D. Thesis, The Pennsylvania State University (1983).

data on the weather profiles at Fort Campbell, no firm conclusion can be reached on whether this mechanism could produce the excess attenuation observed.

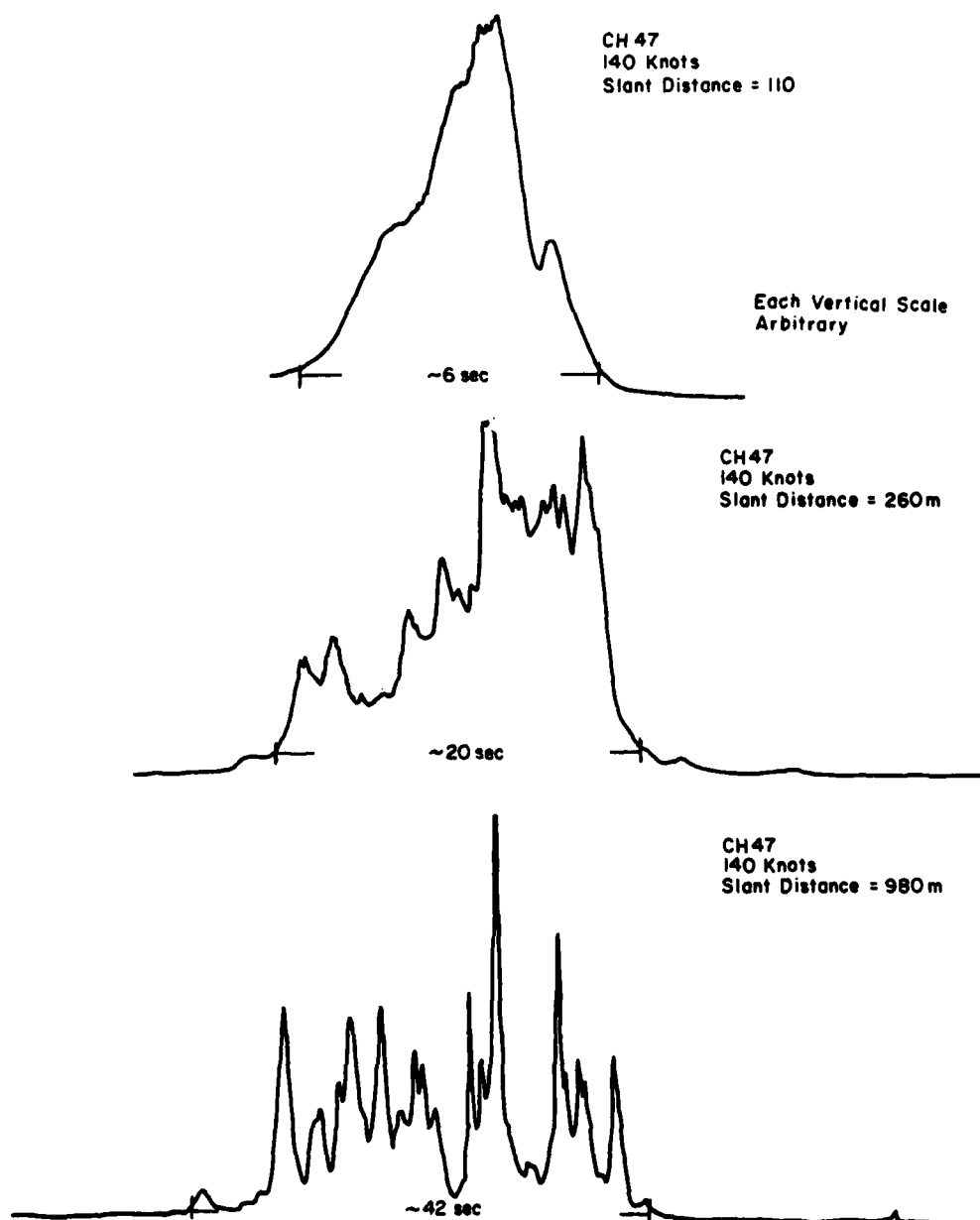


Figure 24. Flyby variation with slant distance.

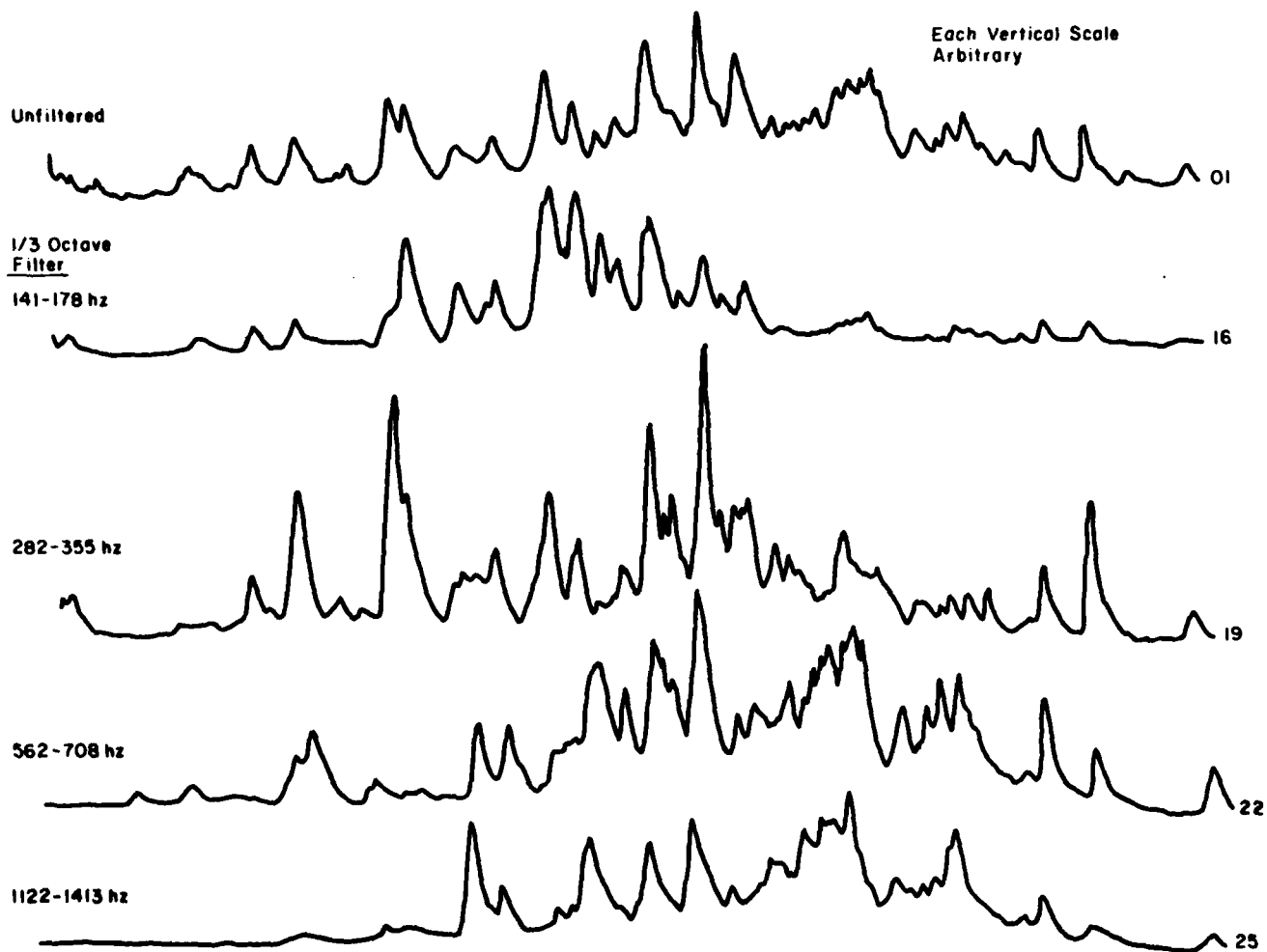


Figure 25. UH-1H flyby profile resolved into frequency bands.

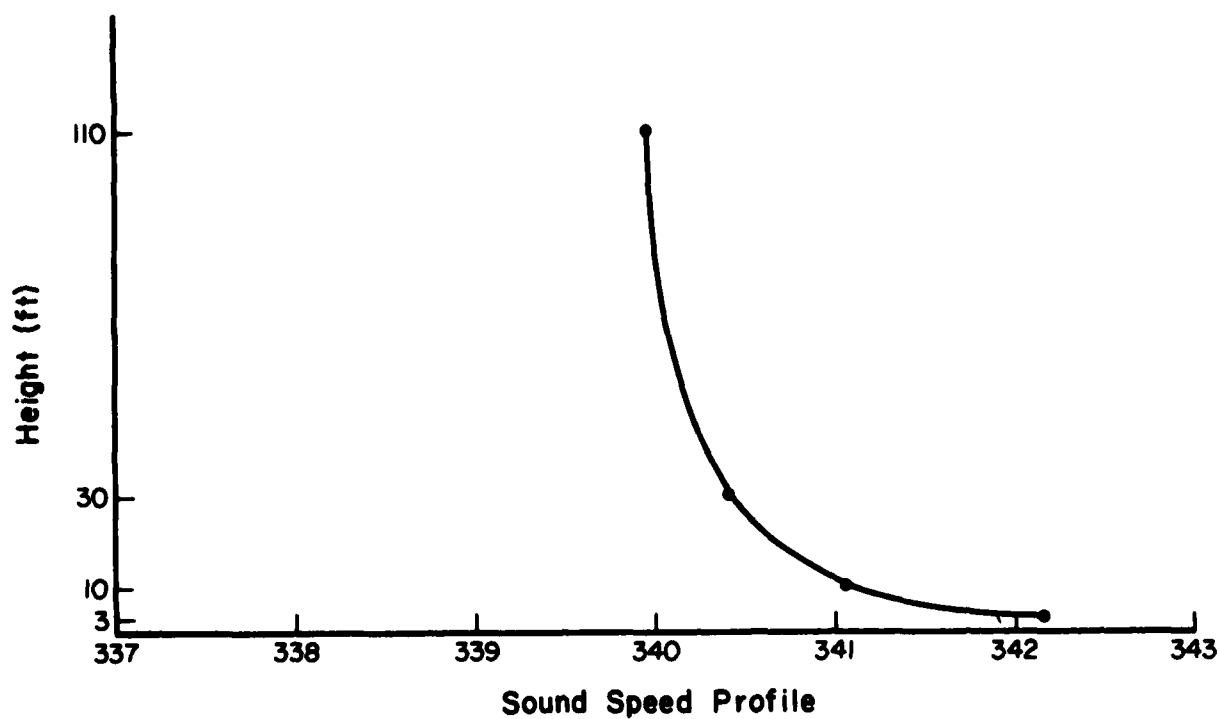
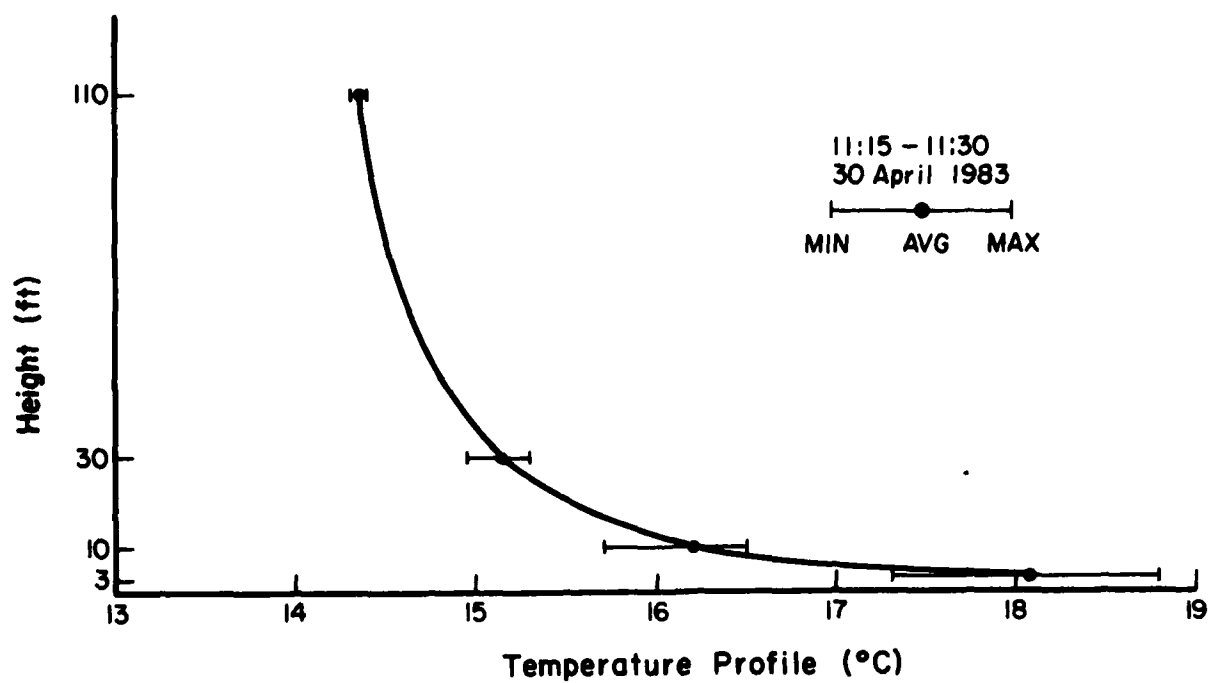


Figure 26. Temperature and sound speed profile at Bondville Field Station.

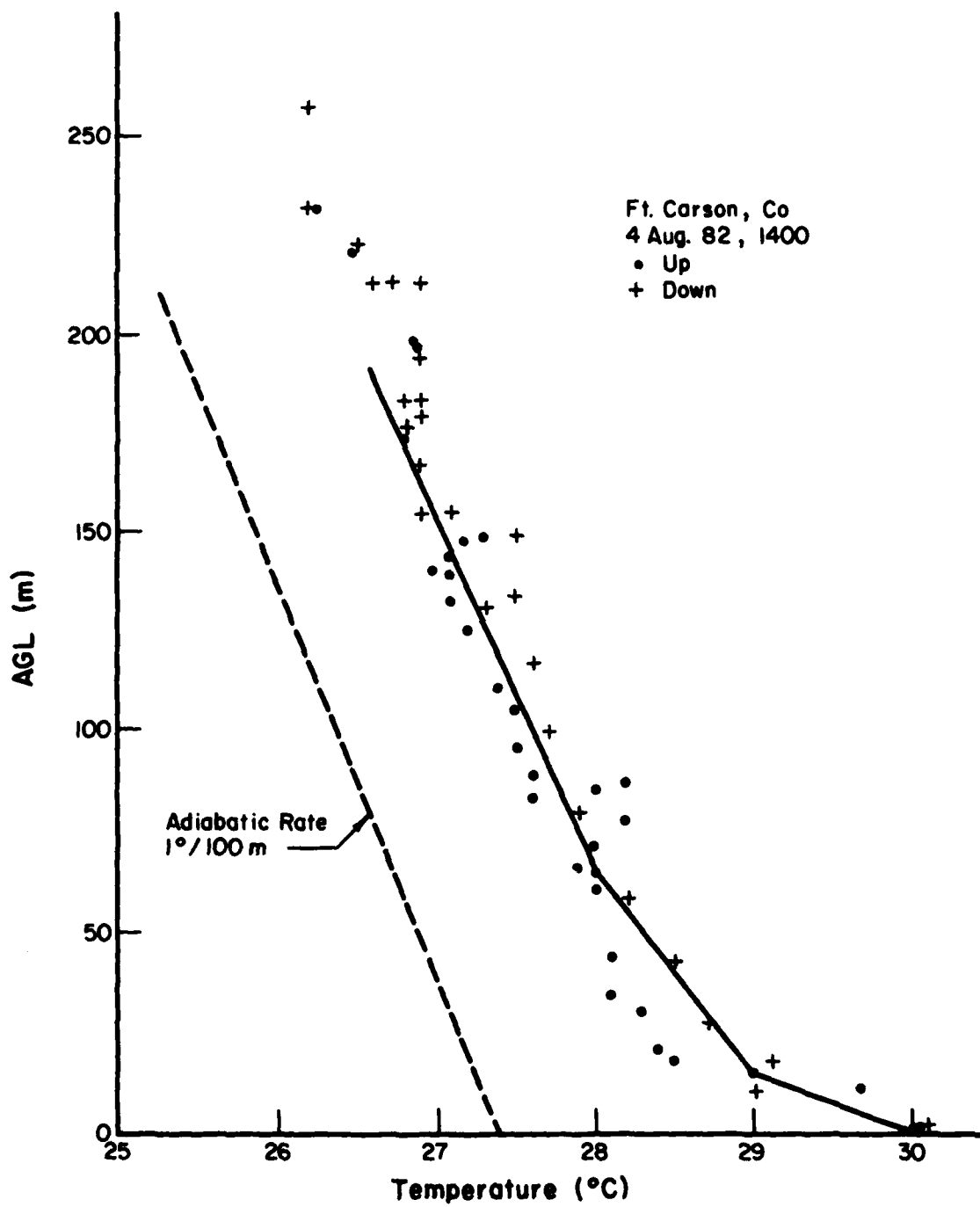


Figure 27. Temperature profile at Fort Carson on 4 August 1982.

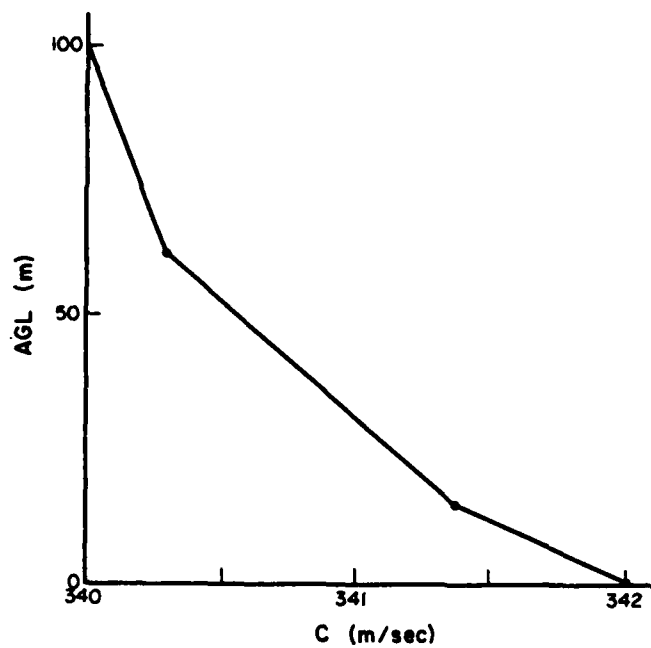


Figure 28. Sound speed profile at Fort Carson on 4 August 1982.

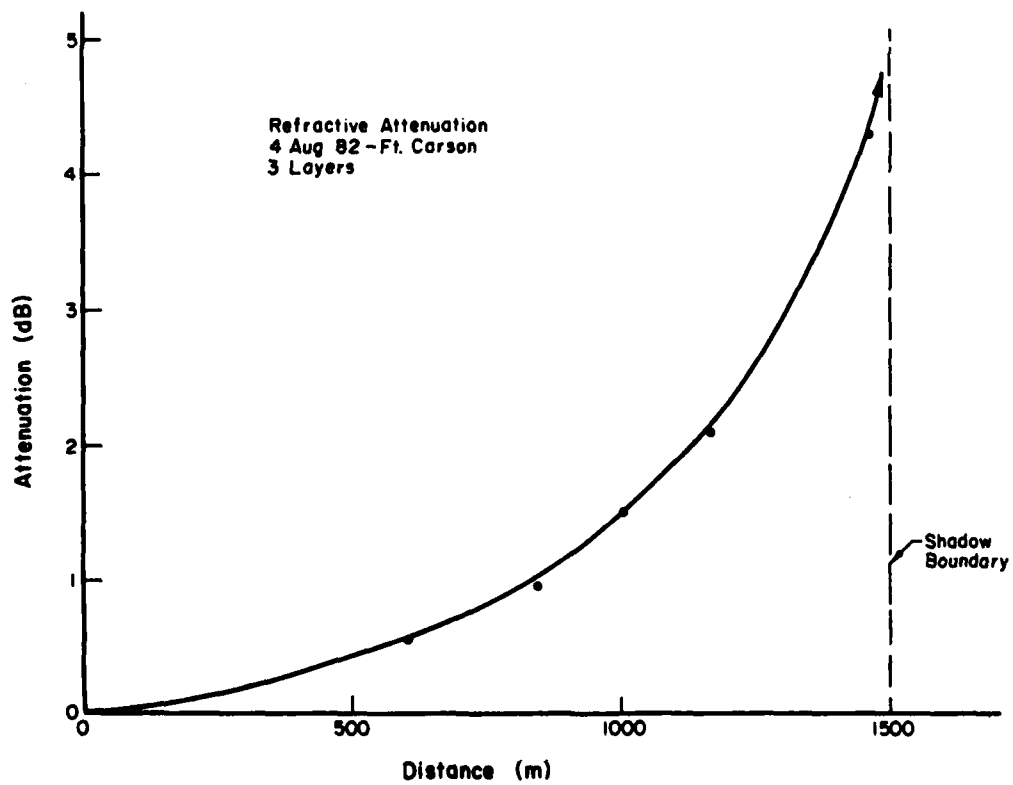


Figure 29. Refractive attenuation at Fort Carson on 4 August 1982.

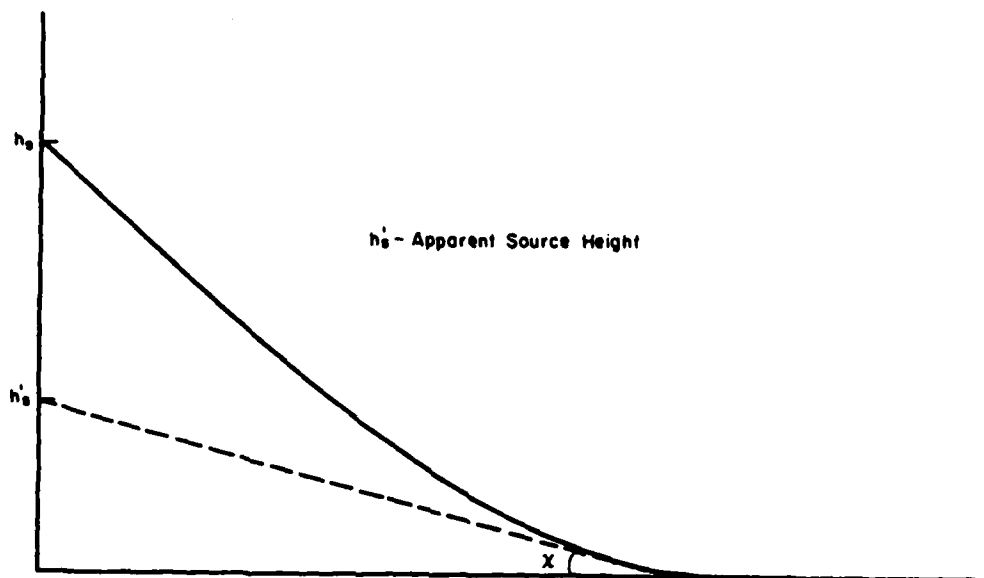


Figure 30. Apparent source height at Fort Carson on 4 August 1982.

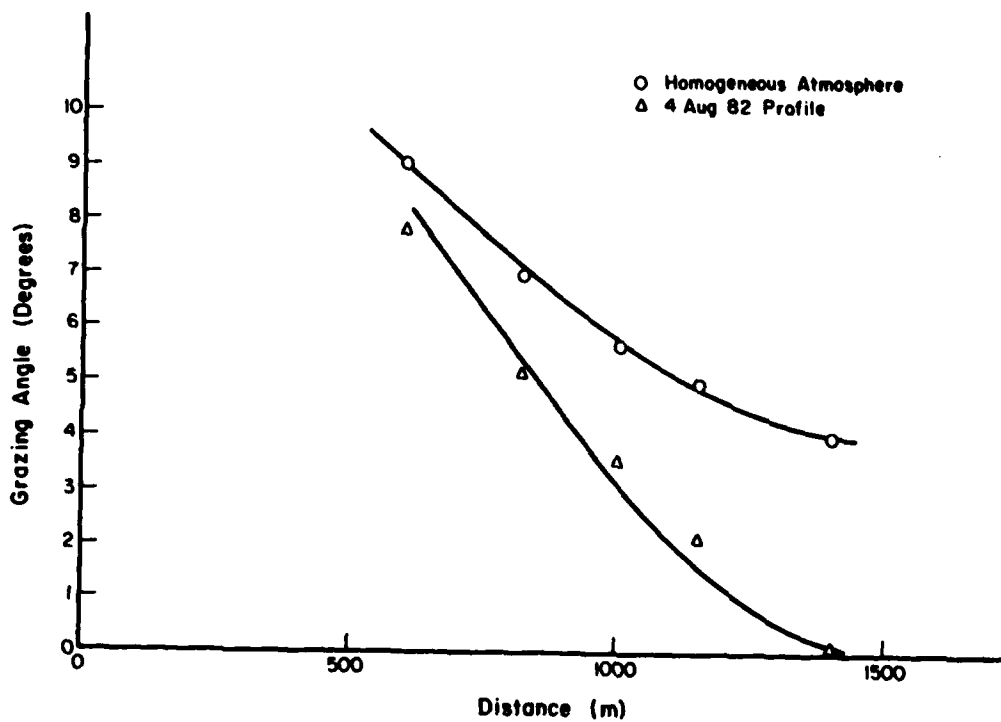


Figure 31. Comparison of grazing angle for a homogeneous atmosphere and the Fort Carson 4 August 1982 profile.

7 CONCLUSIONS AND RECOMMENDATIONS

The FAA procedure has been studied to determine if it can make accurate predictions for rotary-wing aircraft noise decay with distance. It was concluded that the FAA procedure is accurate for aircraft altitudes above 100 m out to a slant distance of 500 m.

The physical mechanisms of sideline noise decay were examined by comparing measured sideline noise levels with those predicted using a detailed computer model that incorporates all known mechanisms. ANSI versus SAE atmospheric attenuation standards were also compared.

A sensitivity analysis was performed to study the effects of known variables on sideline decay. These included:

1. Hard surface versus finite impedance surface.
2. Coherent versus incoherent interference of direct and reflected sound
3. Aircraft type
4. Aircraft airspeed.

The soft coherent model proved most accurate. However, this model still underpredicted levels for slant distances greater than 500 m.

Some unexplained mechanism contributes to sound attenuation. Atmospheric refraction has been suggested as one possible explanation for this result. Work should continue to identify which additional mechanism is increasing sound attenuation.

Standard methods were found suitable for predicting propagation at moderate slant ranges and for high-altitude flights. At lower altitudes, the detailed model should be used to generate SEL versus distance curves.

REFERENCES

- American National Standard Method for the Calculation of the Absorption of Sound by the Atmosphere, ANSI S1.26 (American National Standards Institute, 1978).
- AR 200-1, Environmental Protection and Enhancement (Department of the Army, 15 June 1982).
- Attenborough, Keith, Sabih I. Hayeh, and James M. Lawther, "Propagation of Sound Above a Porous Half Space," J. Acoust. Soc. Am., Vol 68, No. 5 (November 1980), pp 1493-1501.
- Brown, E. H. and S. F. Clifford, "On the Attenuation of Sound by Turbulence," J. Acoust. Soc. Am., Vol 60, No. 4 (1976).
- Daigle, G. A., J. E. Piercy, and T. F. W. Embleton, "Effects of Atmospheric Turbulence on the Interference of Sound Waves Near the Boundary," J. Acoust. Soc. Am., Vol 64, No. 2 (1978).
- Donato, R. J., "Propagation of a Spherical Wave Near a Plane Boundary with a Complex Impedance," J. Acoust. Soc. Am., Vol 60, No. 1 (July 1976), pp 34-39.
- Hayes, Wallace D., Rudolf C. Haefeli, and H. E. Karlsrud, Sonic Boom Propagation in a Stratified Atmosphere, With Computer Program, NASA Contractor Report CR-1299 (National Aeronautics and Space Administration, 1969).
- Homans, B., L. Little, and P. Schomer, Rotary-Wing Aircraft Operational Noise Data, Technical Report N-38/ADA051999 (U.S. Army Construction Engineering Research Laboratory [USA-CERL], February 1978).
- Newman, J. Steven, Edward J. Rickley, and Tyrone L. Bland, Helicopter Noise Exposure Curves for Use in Environmental Impact Assessments, DOT-FAA-EE-82-16 (Department of Transportation, Federal Aviation Administration, Office of Environment and Energy, 1982).
- Paterson, Robert W. and Ray U. Amiet, Noise of a Model Helicopter Rotor Due to Ingestion of Turbulence, NASA Contractor Report 3213 (National Aeronautics and Space Administration, 1979).
- Pernet, D. F. The Effect of Small Variations in the Height of a Microphone Above Ground Surface on the Measurement of Aircraft Noise, Acoustics Report AC77 (National Physical Laboratory, October 1976).
- Roth, S. David, Acoustic Propagation in the Surface Layer Under Convectively Unstable Conditions, Ph.D. Thesis, The Pennsylvania State University (1983).
- Schomer, P. D. and B. L. Homans, Technical Background: Interim Criteria for Planning Rotary-Wing Aircraft Patterns and Siting Noise Sensitive Land Uses, Interim Report N-9/ADA031449 (USA-CERL, September 1976).

Schomer, P. D. and B. L. Homans, User Manual: Interim Procedure for Planning Rotary-Wing Aircraft Traffic Patterns and Siting Noise Sensitive Land Uses, Interim Report N-10/ADA031450 (USA-CERL, September 1976).

Schomer, P. D., A. Averbuch, M. W. Weisberg, R. Brown, and L. M. Little, True-Integrating Environmental Noise Monitor and Sound Exposure Level Meter, USA-CERL TR N-41/ADA060958 (USA-CERL, May 1978).

Schomer, P. D., A. Averbuch, and R. Raspet, Operational Noise Data for UH-60A and CH-47C Army Helicopters, Technical Report N-131/A118796 (USA-CERL, July 1982).

Speakman, Jerry D., Effect of Propagation Distance on Aircraft Flyover Duration, AFAMRL-TR-81-28 (U.S. Air Force Aerospace Medical Research Laboratory, 1981).

Standard Values of Atmosphere Absorption as a Function of Temperature and Humidity, ARP 866A (Society of Automotive Engineers, 1975).

CERL DISTRIBUTION

Chief of Engineers
ATTN: Tech Monitor
ATTN: DAEN-ASI-L (2)
ATTN: DAEN-CCP
ATTN: DAEN-CW
ATTN: DAEN-CWE
ATTN: DAEN-CWM-R
ATTN: DAEN-CWO
ATTN: DAEN-CWP
ATTN: DAEN-EC
ATTN: DAEN-ECC
ATTN: DAEN-ECE
ATTN: DAEN-ZCF
ATTN: DAEN-ECR
ATTN: DAEN-RD
ATTN: DAEN-RDC
ATTN: DAEN-RDM
ATTN: DAEN-RM
ATTN: DAEN-ZCZ
ATTN: DAEN-ZCE
ATTN: DAEN-ZCI
ATTN: DAEN-ZCM

FESA, ATTN: Library 22060
ATTN: DET III 79906

US Army Engineer Districts
ATTN: Library (41)

US Army Engineer Divisions
ATTN: Library (14)

US Army Europe
AEAE-ODCS/Engr 09403
ISAE 09081

V Corps
ATTN: DEH (11)

VII Corps
ATTN: DEH (15)

21st Support Command
ATTN: DEH (12)

USA Berlin
ATTN: DEH (11)

USASETAF
ATTN: DEH (10)
Allied Command Europe (ACE)
ATTN: DEH (3)

8th USA, Korea (19)

ROK/US Combined Forces Command 96301
ATTN: EUSA-HHC-CFC/Engr

USA Japan (USARJ)
ATTN: AJEN-PE 96343
ATTN: DEH-Honshu 96343
ATTN: DEH-Okinawa 96331

Area Engineer, AEDC-Area Office
Arnold Air Force Station, TN 37389

416th Engineer Command 60623
ATTN: Facilities Engineer

US Military Academy 10966
ATTN: Facilities Engineer
ATTN: Dept of Geography &
Computer Science
ATTN: DSCPER/MAEN-A

AMMRC, ATTN: DRXMR-WZ 02172

USA ARRCOM 61299
ATTN: DRCIS-RI-I
ATTN: DRSAR-IS

DARCOM - Dir., Inst., & Svcs.
ATTN: DEH (23)

DLA ATTN: DLA-WI 22314

DNA ATTN: NADS 20305

FORSCOM
FORSCOM Engineer, ATTN: APEN-DEH
ATTN: DEH (23)

HSC
ATTN: HSLO-F 78234
ATTN: Facilities Engineer
Pittsmons AMC 80240
Walter Reed AMC 20012

INSCOM - Ch, Instl. Div.
ATTN: Facilities Engineer (3)

MDW
ATTN: DEH (3)

MTMC
ATTN: MTMC-SA 20315
ATTN: Facilities Engineer (3)

NARADCOM, ATTN: DRDNA-F 01760

TARCOM, Fac. Div. 48090

TRADOC
HQ, TRADOC, ATTN: ATEN-DEH
ATTN: DEH (19)

TSARCOM, ATTN: STSAS-F 63120

USACC
ATTN: Facilities Engineer (2)

WESTCOM
ATTN: DEH
Fort Shafter 96858
ATTN: APEN-IM

SHAPE 09055
ATTN: Survivability Section, CCB-OPS
Infrastructure Branch, LANDA

HQ USEUCOM 09128
ATTN: ECJ 4/7-LOE

Fort Belvoir, VA 22060 (7)
ATTN: Canadian Liaison Officer
ATTN: Water Resources Support Center
ATTN: Engr Studies Center
ATTN: Engr Topographic Lab
ATTN: ATZA-DTE-SU
ATTN: ATZA-DTE-EM
ATTN: R&D Command

CRAEL, ATTN: Library 03755

WES, ATTN: Library 39180

HQ, XVIII Airborne Corps and
Ft. Bragg 28307
ATTN: AFZA-PE-EE

Chanute AFB, IL 61868
3345 CES/DE, Stop 27

Norton AFB CA 92409
ATTN: AFRC-EX/DEE

Tyndall AFB, FL 32403
AFESC/Engineering & Service Lab

NAFAC
ATTN: RDT&E Liaison Office (6)
ATTN: Sr. Tech. FAC-OST 22332
ATTN: Asst. CDR R&D, FAC-03 22332

NCEL 93041
ATTN: Library (Code L08A)

Defense Technical Info. Center 22314
ATTN: DDA (12)

Engineering Societies Library
New York, NY 10017

National Guard Bureau 20310
Installation Division

US Government Printing Office 22304
Receiving Section/Depository Copies (2)

US Army Env. Hygiene Agency
ATTN: HSHB-E 21010

National Bureau of Standards 20760

ENA Team Distribution

Chief of Engineers
ATTN: DAEN-ECC-E
ATTN: DAEN-ECE-B
ATTN: DAEN-ECE-1 (2)
ATTN: DAEN-ZCF-B
ATTN: DAEN-ECZ-A
ATTN: DAEN-ZCE-D (2)

US Army Engineer District
New York 10007
ATTN: Chief, Design Br
Philadelphia 19106
ATTN: Chief, NAPEN-E
Baltimore 21203
ATTN: Chief, Engr Div
Norfolk 23510
ATTN: Chief, NAOEN-D
Huntington 25721
ATTN: Chief, ORHED
Wilmington 28401
ATTN: Chief, SAMEN-D
Savannah 31402
ATTN: Chief, SASAS-L
Mobile 36628
ATTN: Chief, SAMEN-D
Louisville 40201
ATTN: Chief, Engr Div
St. Paul 55101
ATTN: Chief, ED-D
Chicago 60604
ATTN: Chief, NCCPE-PES
Rock Island 61201
ATTN: Chief, Engr Div
St. Louis 63101
ATTN: Chief, ED-D
Omaha 68102
ATTN: Chief, Engr Div

New Orleans 70160
ATTN: Chief, LMNED-DG
Little Rock 72203
ATTN: Chief, Engr Div
Tulsa 74102
ATTN: Chief, Engr Div
Ft. Worth 76102 (3)
ATTN: Chief, SMFED-D
San Francisco 94105
ATTN: Chief, Engr Div
Sacramento 95814
ATTN: Chief, SPKED-D
Far East 96301
ATTN: Chief, Engr Div
Seattle 98124
ATTN: Chief, EN-DB-ST
Walla Walla 99362
ATTN: Chief, Engr Div
Alaska 99501
ATTN: Chief, NPASA-R

US Army Engineer Division
New England 02154
ATTN: Chief, NEDED-T
North Atlantic 10007
ATTN: Chief, NAOEN-T
Middle East (Rear) 22601
ATTN: Chief, MEDED-T
South Atlantic 30303
ATTN: Chief, SAOEN-TS
Huntsville 35807
ATTN: Chief, HNOED-CS
ATTN: Chief, HNOED-SR
Ohio River 45201
ATTN: Chief, Engr Div
Missouri River 68101
ATTN: Chief, MRDED-T
Southwestern 75202
ATTN: Chief, SWDED-T
South Pacific 94111
ATTN: Chief, SPDED-TG
Pacific Ocean 96858
ATTN: Chief, Engr Div
North Pacific 97208

6th US Army 94129
ATTN: AFKC-EN

7th Army Combined Arms Trng. Cntr. 09407
ATTN: AETTM-HRD-END

Armament & Dev. Command 21005
ATTN: DRDAR-BLT

US Army Tank Command
ATTN: DRSTA-SP 48090

USA ARRADCOM 07801
ATTN: DRDAR-LCA-OK

DARCOM 22333
ATTN: DRCPA-E
ATTN: DRCIS-A

TRADOC
Ft. Monroe, VA 23651

Ft. Clayton, Canal Zone 34004
ATTN: DFAE

Ft. Detrick, MD 21701

Ft. Leavenworth, KS 66027
ATTN: ATZLCA-SA

Ft. McPherson, GA 30330 (2)

Ft. Monroe, VA 23651 (6)

Ft. Rucker, AL 36360 (2)

Aberdeen Proving Ground, MD 21005
ATTN: DRDAR-BLL
ATTN: STEAP-MT-E

Human Engineering Lab. 21005 (2)

USA-WES 39181

Army Environmental Hygiene Agency 21005

Naval Air Station 92135
ATTN: Code 661

NAVFAC 22332 (2)

Naval Air Systems Command 20360

US Naval Oceanographic Office 39522

Naval Surface Weapons Center 22485
ATTN: N-43

Naval Undersea Center, Code 401 92152 (2)

Bolling AFB, DC 20332
AF/LEEEU

Patrick AFB, FL 32925
ATTN: XRQ

Tyndall AFB, FL 32403
AFESC/TST

Wright-Patterson AFB, OH 45433 (3)

Building Research Advisory Board 20418

Transportation Research Board 20418

Dept of Housing and Urban Development 20410

Dept of Transportation Library 20590

Illinois EPA 62706 (2)

Federal Aviation Administration 20591

Federal Highway Administration 22201
Region 15

NASA 23365 (2)

National Bureau of Standards 20234

Office of Noise Abatement 20590
ATTN: Office of Secretary

USA Logistics Management Center 23801

Airports and Construction Services Dir
Ottawa, Ontario, Canada K1A 0N8

Division of Building Research
Ottawa, Ontario, Canada K1A 0R6

National Defense HQDA
Ottawa, Ontario, Canada K1A 0K2

USAAATCA
ATTN: Aeronautical Servs. Ofc.

Raspet, Richard

Prediction and modeling of helicopter noise / by Richard Raspet, Mark Kief, Raymond Daniels. - Champaign, Ill : Construction Engineering Research Laboratory, 1984.

52 p. (Technical report ; N-186)

1. Helicopters-noise. I. Kief, Mark. II. Daniels, Raymond. III. Title. IV. Series ; Technical report (Construction Engineering Research Laboratory) : N-186.

END

FILMED

10-84

DTIC